Practical naturalness and its implications for weak scale supersymmetry

Howard Baer[1,*] Vernon Barger[2,†] Dakotah Martinez[1,‡] and Shadman Salam[3,§]

[1]*Homer L. Dodge Department of Physics and Astronomy, University of Oklahoma, Norman, Oklahoma 73019, USA*

[2]*Department of Physics, University of Wisconsin, Madison, Wisconsin 53706, USA*

[3]*Center for Mathematical Sciences, Department of Mathematics and Natural Sciences, Brac University, Dhaka 1212, Bangladesh*

(Received 5 June 2023; accepted 12 August 2023; published 29 August 2023)

We revisit the various measures of practical naturalness for models of weak-scale supersymmetry (SUSY) including: 1. electroweak (EW) naturalness; 2. naturalness via sensitivity to high-scale (HS) parameters [Ellis-Enquist-Nanopoulos-Zwirner/Barbieri-Giudice (EENZ/BG)]; 3. sensitivity of Higgs soft terms due to high-scale radiative corrections; and 4. stringy naturalness (SN) from the landscape. The EW measure is most conservative and seems unavoidable. We debut a new numerical routine for calculating the EENZ/BG measure from any SUSY Les Houches Accord file. We implement a careful analysis and comparison of these measures in the mSUGRA/CMSSM and NUHMi model parameter spaces and via parameter-space scans. We demonstrate the reasoning behind why—and the extent to which—the EENZ/BG and HS measures overestimate the degree of fine-tuning. We find the overestimation can range up to a factor of over 1000. While EENZ/BG and HS have ambiguities when applied to models such as anomaly- and mirage-mediation, the EW measure has no such ambiguity and so we display the natural parameter space regions of these models. SN depends on the landscape distribution of soft terms, but is closely related to EW naturalness via the atomic principle.

DOI: 10.1103/PhysRevD.108.035050

I. INTRODUCTION

Weak-scale supersymmetry (SUSY) provides a solution to the hierarchy of scales problem [1,2] of particle physics and is supported by data from four different virtual effects[1]:

(1) The successful running of gauge couplings to unified values within the minimal supersymmetric Standard Model (MSSM) [3–6];
(2) The predicted large value of the top-quark mass needed for radiatively-induced electroweak symmetry breaking (REWSB) [7–9];
(3) The match between the narrow theory-predicted window of m_h values within the MSSM and the subsequent Higgs boson discovery [10];
(4) Precision electroweak corrections which, in the m_t vs m_W plane, actually favor heavy SUSY over the Standard Model (SM) [11].

In addition, some remnant SUSY is expected to survive superstring compactification from 10/11 to four spacetime dimensions on a Calabi-Yau manifold [12]. In fact, it is conjectured that the landscape of all geometric, stable, string/M theory compactifications to Minkowski spacetime (at leading order) are supersymmetric [13]; manifolds which do not respect these conditions typically lead to Witten bubble-of-nothing instabilities. Also, in contrast to the SM, SUSY leads to EW vacuum stability at ultrahigh energies owing to gauge sector contributions (D-terms) to Higgs quartic couplings [14]. Moreover, highly motivated SM extensions which introduce a new high-energy scale—such as the inclusion of see-saw neutrinos or a Peccei-Quinn (PQ) sector to solve the strong CP problem—avoid the Higgs mass blow-up due to the introduced new high-mass scales [15–17] unless the underlying model is supersymmetric. With respect to the axion solution to the strong CP problem, intrinsically supersymmetric discrete R-symmetries [18], which are expected to emerge from string compactifications [19], provide an avenue for emergence of

[*]baer@ou.edu
[†]barger@pheno.wisc.edu
[‡]dakotah.s.martinez-1@ou.edu
[§]ext.shadman.salam@bracu.ac.bd

[1]Radiative corrections have historically been a reliable guide to new physics and (as just a few examples) indeed have presaged the discovery of the W and Z vector bosons, the top quark and the Higgs bosons.

the required global $U(1)_{PQ}$ symmetry with sufficient precision as to solve the axion-quality problem [20,21]. In such models, the PQ scale f_a is related to the hidden-sector SUSY breaking scale

$$m_{\mathrm{hidden}} \sim f_a \sim 10^{11}\ \mathrm{GeV},$$

so that f_a lies within the appropriate cosmological window for axion production via coherent oscillations in the early Universe [20]. String instanton effects on the axion quality are also ameliorated within the MSSM [22]. While there are few compelling mechanisms for successful baryogenesis left within the rubric of the SM, the introduction of SUSY leads to several new and/or improved mechanisms to address the matter-antimatter asymmetry [23,24].

In spite of this litany of successes, it is common at this time to dismiss weak-scale supersymmetry (WSS) [25] as a viable beyond-the-Standard Model (BSM) theory due to the apparent lack of new physics signals at the CERN Large Hadron Collider (LHC) [26]. The data from LHC, which is by-and-large in accord with SM expectations [27], is in contrast to early theoretical expectations for WSS based upon naturalness arguments that superpartners would emerge with mass values not far from the weak scale [28–36]

$$m_{\mathrm{weak}} \simeq m_{W,Z,h} \sim 100\ \mathrm{GeV}.$$

At present, such arguments are being used to set policy and guide future facilities for the high-energy physics (HEP) frontier [37,38]. Given these crucial factors, it is essential to go back and review the naturalness-based arguments to assess when and where and if they present a reliable guide to the search for new physics, as the original naturalness arguments are more than 30 years old, and numerous insights have lead to greater clarity in the present time.

In this paper, we revisit several proposed naturalness measures which have been applied to various supersymmetric models. As opposed to 't Hooft naturalness, these measures determine the degree of what is defined in Sec. III as practical naturalness; that all independent contributions to some observable $\mathcal{O}$ are comparable to, or less than, $\mathcal{O}$. Historically, the first of these is the Ellis-Enquist-Nanopoulos-Zwirner/Barbieri-Giudice (EENZ/BG) [28,29] measure (labeled here as Δ_{BG}) which determines the sensitivity of the measured value of the weak scale to variation in model parameters p_i (i indexes the various parameters under consideration). Conventionally the p_i have been taken to be the various soft SUSY breaking terms starting at a high effective field theory (EFT) cutoff scale

$$\Lambda = m_{\mathrm{GUT}} \simeq 2 \times 10^{16}\ \mathrm{GeV}.$$

This Δ_{BG} measure associates a numerical value to Susskind's definition of naturalness [39],

$$\Delta_{\mathrm{BG}} \equiv \max_i \left| \frac{\partial \log m_Z^2}{\partial \log p_i} \right| = \max_i \left| \frac{p_i}{m_Z^2} \frac{\partial m_Z^2}{\partial p_i} \right|. \tag{1}$$

For small $\Delta_{\mathrm{BG}} \lesssim 30$, then sparticle masses are expected to lie below the several hundred GeV range, although in some special regions of model parameter space, such as the focus point region [40,41] of the minimal supergravity (mSUGRA) [42], or constrained MSSM (CMSSM) [43], multi-TeV scale top squarks can be allowed. Despite its popularity, this measure has been argued to overestimate fine-tuning in SUSY models by large factors and to give ambiguous answers depending on exactly which parameters are chosen to be the fundamental p_i [44,45].

A second measure, which we label here as Δ_{HS} (for high-scale sensitivity of the up-Higgs soft mass $m_{H_u}^2$), starts with the approximate SUSY-Higgs mass relation

$$m_h^2 \sim \mu^2 + m_{H_u}^2(\mathrm{weak}),$$

where

$$m_{H_u}^2(\mathrm{weak}) = m_{H_u}^2(\Lambda) + \delta m_{H_u}^2.$$

One then requires

$$\Delta_{\mathrm{HS}} = \delta m_{H_u}^2 / m_h^2 \tag{2}$$

to be small. This measure, which is inconsistent with Δ_{BG} in that it doesn't allow for multi-TeV top squarks even in the focus point (FP) region, has led to intense scrutiny of LHC top-squark searches. This is because it is expected that [46–52]

$$\delta m_{H_u}^2 \sim \frac{6 f_t^2}{(4\pi)^2} m_{\tilde{t}}^2 \log \frac{\Lambda^2}{m_{\tilde{t}}^2}.$$

Δ_{HS} was found to lead to violations of the fine-tuning rule [44]; it is not allowed to claim fine-tuning amongst dependent terms which contribute to some observable $\mathcal{O}$. (As mentioned earlier, it is the large top-quark Yukawa coupling f_t which radiatively drives $m_{H_u}^2$ from its large SUGRA value at the high scale to negative values at the weak scale so that the EW symmetry is spontaneously broken.) In this case, $\delta m_{H_u}^2$ and $m_{H_u}^2(\Lambda)$ are dependent, leading to overestimates in fine-tuning.

A third measure is the electroweak measure Δ_{EW} [53,54] which is touted to be more conservative and model independent than the others, and also unavoidable (within the context of the MSSM). It is based on the SUSY-Higgs potential-minimization condition

$$\begin{aligned} m_Z^2/2 &= \frac{m_{H_d}^2 + \Sigma_d^d - (m_{H_u}^2 + \Sigma_u^u)\tan^2\beta}{\tan^2\beta - 1} - \mu^2 \\ &\simeq -m_{H_u}^2 - \mu^2 - \Sigma_u^u(\tilde{t}_{1,2}), \end{aligned} \tag{3}$$

where all right-hand-side entries are taken as their weak-scale values and

$$\Delta_{\mathrm{EW}} \equiv \max_i |\text{entries on rhs of Eq. (3)}| / (m_Z^2/2). \tag{4}$$

This measure was preceded by Chan *et al.* [55] who suggested that the magnitude of the SUSY-conserving μ parameter could serve as a fine-tuning measure all by itself. This measure is sometimes criticized in that it apparently lacks sensitivity to high-scale parameters, which we will expand upon later.

A fourth entry is not at present a quantifiable measure, but known nonetheless as stringy naturalness (SN), and arises from Douglas' consideration of the string landscape picture [56]:

A. Stringy naturalness

An observable $\mathcal{O}_1$ is more (stringy) natural than an observable $\mathcal{O}_2$ if more phenomenologically viable string vacua lead to $\mathcal{O}_1$ than to $\mathcal{O}_2$.

To quantify stringy naturalness, at least two ingredients are needed:

(1) The expected distribution of some quantity within the landscape of vacua possibilities and
(2) An anthropic selection ansatz for which many choices would lead to universes that are unable to support observers.

For the case of SUSY models, the first of these is usually how soft terms are distributed in the landscape while the second of these is the magnitude of the weak scale itself; if the predicted value of $m_{\rm weak}$ within each pocket universe is too far displaced from its measured value in our Universe, then nuclear physics no longer can support atoms as we know them, leading to no complex chemistry as seems to be needed for observers [57]. This principle is known as the atomic principle. An attempt to compute and display stringy naturalness via density of dots in model parameter space has been made in Ref. [58].

In the present work, we reexamine these several measures of naturalness, filling in some of the many gaps of understanding that exist in the literature. Part of our work is based on a new computation of $\Delta_{\rm BG}$ naturalness based on a numerical evaluation of the derivatives in Eq. (1). This new computation is embedded in the publicly available code DEW4SLHA [54] so that the updated code can provide values of each of the measures $\Delta_{\rm BG}$, $\Delta_{\rm HS}$, and $\Delta_{\rm EW}$ given an input SUSY Les Houches Accord (SLHA) file [59].[2] Thus, another reason to revisit the fine-tuning issue is that we have developed a code which allows for detailed comparison of all three measures which goes beyond previous semianalytic techniques that gave explicit results only for certain fixed $\tan\beta$ values. Now we are able to compute ratios of naturalness measures to determine the extent to which some measures can overestimate fine-tuning in SUSY models. For instance, in the SUSY theory review contained in the Particle Data Book [60], it is suggested that the overestimates may range up to a factor of 10; in contrast, we find overestimates ranging up to factors of over 1000.

The remainder of this paper is organized as follows. In Sec. II, we review two paradigmatic models mSUGRA/CMSSM and NUHMi which are typically associated with gravity-mediated SUSY breaking. In Sec. III we define what we mean by naturalness and practical naturalness. In Sec. IV we show how the three naturalness measures arise from practical naturalness and we highlight the model dependence of the EENZ/BG measure; we also introduce our new numerical routine to evaluate the EENZ/BG value from any SUSY Les Houches Accord file. In Sec. V, we compare and contrast the various measures in mSUGRA/CMSSM and NUHMi model parameter space while in Sec. VI we compute ratios of measures and show that $\Delta_{\rm BG}$ and $\Delta_{\rm HS}$ can overestimate fine-tuning by up to three orders of magnitude compared to $\Delta_{\rm EW}$. In Sec. VII we emphasize ambiguities in evaluating $\Delta_{\rm BG}$ and $\Delta_{\rm HS}$ in anomaly-mediated SUSY breaking models and in Sec. VIII we illustrate the same for mirage mediation. Since there is no ambiguity for $\Delta_{\rm EW}$, we display natural parameter space which satisfies present LHC Higgs and sparticle mass bounds using the EW measure for natural anomaly and mirage mediation. Our summary and conclusions are contained in Sec. IX.

II. SOME MODELS OF WEAK-SCALE SUSY

Here, we make reference to several SUSY models which we briefly review for the reader.

A. mSUGRA/CMSSM model

Some of our numerical work refers to the mSUGRA [42,61–65] or CMSSM model [43] with parameter space[3]

$$m_0, m_{1/2}, A_0, \tan\beta \quad \text{and} \quad \text{sign}(\mu) \quad (\text{mSUGRA/CMSSM}). \tag{5}$$

In this model, m_0 refers to a unified high-scale scalar soft breaking mass, usually defined at the scale $m_{\rm GUT}$ where the three gauge couplings unify. While unified gaugino masses can be achieved in many supersymmetric models with a simple choice for gauge kinetic function, the scalar-mass unification is an (unmotivated) simplifying assumption that violates expectations from gravity-mediated SUSY breaking models where nonuniversal scalar masses are expected unless imposed by some symmetry [66–68]. For instance, scalar masses within a matter generation may be expected to unify to $m_0(i)$ (for generation index $i = 1$–3) due to the fact that all matter fills out a complete 16-dimensional

[2]The code DEW4SLHA, written by D. Martinez, is available at https://www.dew4slha.com.

[3]We accept that the mSUGRA model and the CMSSM model are two different names for the same model defined by the parameter space in Eq. (5). Indeed, paragraph 2 of the original Kane *et al.* paper [43] lays out the supergravity origins of the CMSSM model.

spinor representation of $SO(10)$. However, generational universality $m_0(1) = m_0(2) = m_0(3)$ is not expected and leads to the famous SUSY flavor and CP problems [69]. Furthermore, the Higgs fields H_u and H_d live in different $SU(5)$ [or general $SO(10)$] representations from matter scalars, and hence are also not expected to unify.

B. Nonuniversal Higgs models

This family of models meets the expectation that

$$m_{H_u} \neq m_{H_d} \neq m_0(i).$$

The simplest case, nonuniversal Higgs models (NUHM1) [70] assumes

$$m_{H_u} = m_{H_d} \neq m_0(i),$$

as expected in simple $SO(10)$ GUTs. Meanwhile, NUHM2 [71–73] satisfies

$$m_{H_u} \neq m_{H_d} \neq m_0(1) = m_0(2) = m_0(3),$$

which occurs in $SU(5)$ or general $SO(10)$ GUTs. In all cases, when we refer to SUSY-GUT models, we particularly emphasize the importance of local grand unification [74] wherein the geography of fields on a string compactified manifold determines the GUT symmetry properties [75,76]. Sometimes an NUHM3 model with

$$m_0(1) = m_0(2) \neq m_0(3)$$

is used [77], and sometimes NUHM4 with

$$m_0(1) \neq m_0(2) \neq m_0(3)$$

is used, especially for discussion of the SUSY-flavor and CP problems [78]. For these NUHMi models ($i = 1$–4), frequently the GUT values of m_{H_u} and m_{H_d} are traded for the weak-scale values of the superpotential μ parameter and the pseudoscalar Higgs mass m_A via the scalar potential minimization conditions. Thus, the NUHMi parameter space is given by

$$m_0(i), m_{1/2}, A_0, \tan\beta, \mu, m_A. \tag{6}$$

The NUHMi models are particularly convenient to explore natural supersymmetry since one can directly restrict oneself to natural values of the μ parameter; $\mu \sim 100$–350 GeV.

In Fig. 1, we plot in the m_0 vs $m_{1/2}$ plane of the NUHM2 model the ratio of $m_{H_u}(m_{\rm GUT})/m_0$ which is needed to ensure that the SUSY μ parameter is fixed at a natural value of $\mu = 200$ GeV. We also adopt $A_0 = -1.6 m_0$ and $\tan\beta = 10$ with $m_A = 2$ TeV. From the plot, we see that

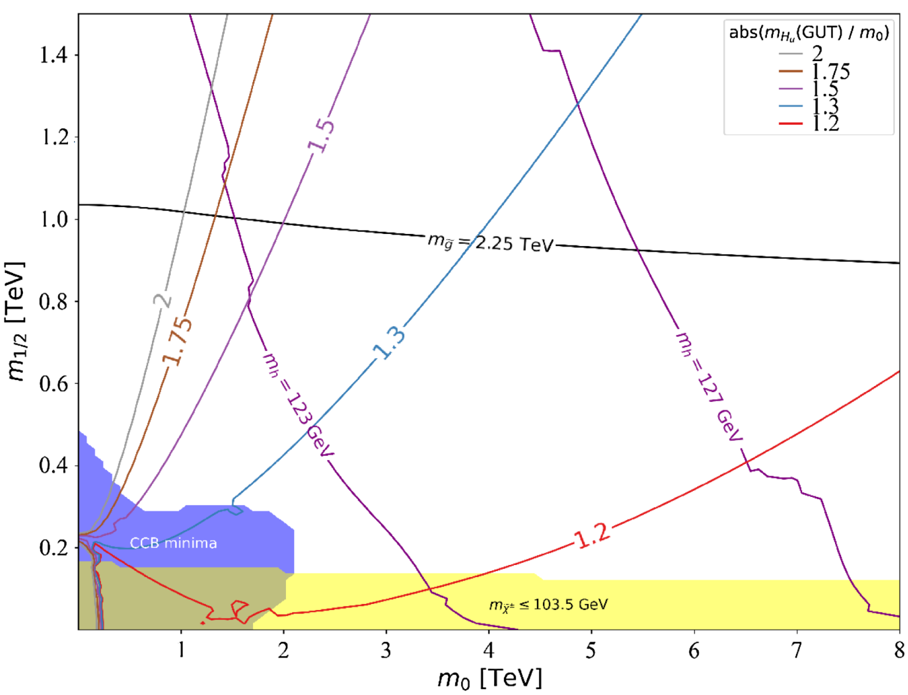

FIG. 1. Ratio of $m_{H_u}(m_{\rm GUT})/m_0$ in the NUHM2 model which is needed to ensure that $\mu = 200$ GeV. We also take $A_0 = -1.6 m_0$ and $\tan\beta = 10$ with $m_A = 2$ TeV. The blue shaded region is excluded, as these points lead to charge-or-color-breaking (CCB) minima. The yellow shaded region near the bottom has the lightest chargino below LEP2 limits, $m_{\tilde\chi_1^\pm} < 103.5$ GeV. The mass spectra are calculated using SOFTSUSY.

$m_{H_u}(m_{\rm GUT}) \sim 2m_0$ along the left-hand side of the plot, but dips to a ratio of about 1.2–1.5 for the bulk of the plane which respects the $m_h \sim 123$–127 GeV range (assuming about a 2 GeV error bar on the m_h theory calculation). Thus, only modest deviations of order 20–50% are required in order ensure one of the most fundamental requirements of naturalness, namely $|\mu| \sim m_{\rm weak}$.

C. Natural anomaly and mirage-mediation models

Later in this paper we shall explore naturalness in anomaly-mediated SUSY breaking (AMSB) [79–81] and mixed modulus-AMSB SUSY models, also known as mirage mediation (MM) [82,83].

III. NATURALNESS AND PRACTICAL NATURALNESS

Supersymmetry offers a 't Hooft technically natural solution [84] to the hierarchy of scales problem in that, as the hidden-sector SUSY-breaking scale $m_{\rm hidden}$ (which determines the magnitude of the soft terms via $m_{\rm soft} \sim m_{3/2} \sim m_{\rm hidden}^2/m_P$ in gravity mediation and hence of the weak scale via the scalar-potential minimization conditions) tends to zero, the model becomes more (super)symmetric. The SUSY solution to this big hierarchy problem (BHP)—stabilizing the weak scale so that it does not blow up to the Planck or GUT scale—is not the naturalness issue which concerns many contemporary SUSY theorists. Indeed, 't Hooft naturalness remains a valid solution to the BHP even for very large gaps $m_{\rm soft} \gg m_{\rm weak}$. Instead, it is the so-called little hierarchy problem (LHP) which is of concern [85,86];

> how can it be that $m_{\rm weak} \sim m_{W,Z,h} \sim 100$ GeV is so much smaller than the soft SUSY breaking terms, which, according to LHC data, are $m_{\rm soft} \gtrsim 1$ TeV (owing to LHC bounds $m_{\tilde g} \gtrsim 2.2$ TeV, $m_{\tilde t_1} \gtrsim 1.1$ TeV, …) [87]?

In addressing the LHP, what is of concern is what we call the notion of practical naturalness (PN) [88][4]:

> An observable
>
> $$\mathcal{O} = o_1 + \cdots + o_n$$
>
> is practically natural if all independent contributions o_i to $\mathcal{O}$ are comparable to or less than $\mathcal{O}$.

(Here, "comparable to" means within a factor of several from the measured value.) Practical naturalness embodies the notion of naturalness that is most often used in successful applications of naturalness. For instance, by requiring the charm-quark mass contribution

$$\Delta m_K(c) \simeq \frac{G_F}{\sqrt{2}} \frac{\alpha}{6\pi} \frac{f_K^2 m_K}{\sin^2\theta_W} \cos^2\theta_C \sin^2\theta_C \frac{m_c^2}{m_W^2} \qquad (7)$$

to be comparable to or less than the measured $K_L - K_S$ mass difference Δm_K, Gaillard and Lee [90] were able to predict $m_c \sim 1.5$ GeV several months before the charm quark was discovered.[5] An essential element of practical naturalness is that the contributions o_i should be independent of one another in the sense that if one of the o_i is varied, then the others do not necessarily vary. For instance, Dirac was bothered by various divergent contributions to perturbative QED observables. However, these were dependent contributions in that if the regulator was varied, the different divergent terms would also vary. One should always first combine dependent terms before evaluating naturalness. Once dependent terms are combined then a measure of naturalness emerges,

$$\Delta \equiv \max_i |o_i|/|\mathcal{O}|. \qquad (8)$$

Using PN, we see that QED perturbation theory is practically natural in that the leading terms are comparable to the measured observables whilst higher-order terms (once dependent terms are combined) are typically much smaller.

IV. SOME MEASURES OF NATURALNESS

A. Sensitivity to high-scale parameters: EENZ/BG naturalness

Historically, the first measure of SUSY model naturalness was proposed by Ellis *et al.* in Ref. [28] (based on Susskind [39]) and subsequently used by Barbieri and Giudice [29] to compute sparticle-mass upper bounds in the mSUGRA/CMSSM model; Eq. (1). The measure purports to compute the sensitivity of the measured value of the weak scale to variation in high-scale parameters p_i. The $\Delta_{\rm BG}$ measure is actually a measure of practical naturalness of the weak scale in the case where

$$m_Z^2 = a_1 p_1 + \cdots + a_n p_n.$$

Let us suppose the jth contribution to m_Z^2 is largest. Then,

$$\Delta_{\rm BG} = \max_i \left| \frac{p_i}{m_Z^2} \frac{\partial m_Z^2}{\partial p_i} \right| = \left| \frac{a_j p_j}{m_Z^2} \right|,$$

in accord with Eq. (8). The various

[4]This is in accord with Veltman's notion of naturalness as presented in Ref. [89]. See also Susskind [39].

[5]It is still a breathtaking exercise to plug in the numbers and see the charm-quark mass emerge.

$$\left|\frac{a_i p_i}{m_Z^2}\right| \equiv c_i$$

terms are labeled sensitivity coefficients [91]. The ambiguity here is in which choice to take as to the free parameters p_i.[6]

The starting point is to express m_Z^2 in terms of weak-scale SUSY parameters as in Eq. (3),

$$m_Z^2 \simeq -2m_{H_u}^2 - 2\mu^2, \tag{9}$$

where the partial equality is obtained for moderate-to-large $\tan\beta$ values and where we assume for now that the radiative corrections are small. To evaluate $\Delta_{\rm BG}$, one needs to know the explicit dependence of $m_{H_u}^2$ and μ^2 on the chosen set of fundamental parameters. Semianalytic solutions to the one-loop renormalization group equations for $m_{H_u}^2$ and μ^2 can be found for instance in Refs. [93,94]. For the case of $\tan\beta = 10$, then [36,91,95]

$$\begin{aligned} m_Z^2 \simeq{}& -2.18\mu^2 + 3.84M_3^2 + 0.32M_3M_2 + 0.047M_1M_3 - 0.42M_2^2 + 0.011M_2M_1 - 0.012M_1^2 - 0.65M_3A_t \\ & - 0.15M_2A_t - 0.025M_1A_t + 0.22A_t^2 + 0.004M_3A_b - 1.27m_{H_u}^2 - 0.053m_{H_d}^2 + 0.73m_{Q_3}^2 + 0.57m_{U_3}^2 \\ & + 0.049m_{D_3}^2 - 0.052m_{L_3}^2 + 0.053m_{E_3}^2 + 0.051m_{Q_2}^2 - 0.11m_{U_2}^2 + 0.051m_{D_2}^2 - 0.052m_{L_2}^2 + 0.053m_{E_2}^2 \\ & + 0.051m_{Q_1}^2 - 0.11m_{U_1}^2 + 0.051m_{D_1}^2 - 0.052m_{L_1}^2 + 0.053m_{E_1}^2, \end{aligned} \tag{10}$$

where all terms on the right-hand side are understood to be GUT-scale parameters. As an example, if we adopt $m_{Q_3}^2$ as a fundamental parameter, then the sensitivity coefficient

$$c_{m_{Q_3}^2} = 0.73\frac{m_{Q_3}^2}{m_Z^2},$$

and for $m_{Q_3} = 3$ TeV, then one finds $c_{m_{Q_3}^2} \simeq 800$ so that $\Delta_{\rm BG} > 800$ and the model is certainly fine-tuned. If instead we declare all scalar masses unified to m_0, then there are large cancellations and instead one finds

$$c_{m_0^2} = 0.013\frac{m_0^2}{m_Z^2} \sim 14.2,$$

a reduction in finetuning by over a factor of 50! Clearly, whether or not soft terms are correlated greatly impacts the evaluation of $\Delta_{\rm BG}$.

1. Numerical routine to compute $\Delta_{\rm BG}$

The evaluation of $\Delta_{\rm BG}$ can be done by approximating the partial derivatives with the method of finite central-difference quotients. That is, for finding the partial derivative with respect to a parameter p_1 of $m_Z^2(p_1, p_2, \ldots, p_n)$, where p_i are the fundamental parameters of the model chosen for evaluating $\Delta_{\rm BG}$, then

$$\frac{\partial m_Z^2(p_1, p_2, \ldots, p_n)}{\partial p_1} \approx \frac{m_Z^2(p_1 + h_1, p_2, \ldots, p_n) - m_Z^2(p_1 - h_1, p_2, \ldots, p_n)}{2h_1}. \tag{11}$$

Here, h_1 is the size of the variation of the differentiation parameter p_1, which is then used to determine the resulting change in m_Z^2. Since this is a partial derivative, all other input parameters are left fixed at their original values prior to differentiation.

To compute this derivative, m_Z^2 must be evaluated in the right-hand side of Eq. (11) as an output of the m_Z^2 Higgs minimization condition, Eq. (3), at the weak-renormalization scale

$$Q_{\rm SUSY} = \sqrt{m_{\tilde t_1} m_{\tilde t_2}}$$

to minimize radiative corrections in the Higgs-minimization condition. For the partial derivative

$$\frac{\partial m_Z^2}{\partial p_i}$$

the GUT-scale parameter p_i is varied to $p_i + h_i$, with $h_i \ll p_i$. Then the new set of GUT-scale parameters,

$$p_1, p_2, \ldots, p_i + h_i, \ldots, p_{n-1}, p_n$$

are evolved from $Q_{\rm GUT}$ down to $Q_{\rm SUSY}$ using the full two-loop MSSM renormalization group equations (RGEs). Lastly, the varied value

[6]Giudice remarks in Ref. [92]; "It may well be that, in some cases, Eq. (1) overestimates the amount of tuning. Indeed, Eq. (1) measures the sensitivity of the prediction of m_Z as we vary parameters in theory space. However, we have no idea how this theory space looks like, and the procedure of independently varying all parameters may be too simple minded." See also discussion in Ref. [34].

$$m_Z^2(p_1, p_2, \ldots, p_i + h_i, \ldots, p_{n-1}, p_n)$$

is computed from the tree-level Higgs minimization condition for m_Z^2, giving a value slightly deviated from 91.2^2. This value is then used in Eq. (11) and the process is repeated for the other direction of variation.

In this numerical derivative approach, two sources of error can enter and alter the results if not controlled; truncation error and roundoff error. Below are some descriptions of these errors and how we minimize them:

(i) Truncation error is the error of approximating the true, analytical derivative of m_Z^2, with an approximating secant line to the m_Z^2 curve in the theory space. For a given derivative variation size of h, the truncation error for a two-point method is suppressed by a term of $\mathcal{O}(h^2)$. This error remains relatively small so long as the step size $h < 1$ and the higher-order derivatives of m_Z^2 are reasonably bounded.

(ii) Roundoff error comes from representing the values $p_1, p_2, \ldots, p_n$, and h_1 in Eq. (11) as floating-point numbers, where the computer must "round off" most decimal values after a certain number of digits due to storage limitations in binary. Because of this, there is a nonzero spacing between two consecutive floating point numbers x and y, and this spacing is called the unit of least precision [denoted ULP(x)]. Careful error analysis reveals that the roundoff error is proportional to the step size used in the evaluation. This roundoff error is then minimized when, for a two-point central difference, the step size h_i for the derivative $\partial m_Z^2/\partial p_i$ is chosen as $h_i \approx [\mathrm{ULP}(p_i)]^{1/3}$. In order for $h_i < 1$ to occur, the $\mathrm{ULP}(p_i)$ must then also be less than unity.

Numerical error may also enter through the numerical solution of the RGEs, though similar numerical considerations can help control these errors as well. With these sources of error in mind, the error in evaluating this derivative will remain small, i.e., $\mathcal{O}(<1)$, so long as $|p_i| \lesssim 10^{15}$ in magnitude for all i. This leads to $h_i < 1$ for double-precision floating point numbers. DEW4SLHA offers the option of performing this calculation with even higher-accuracy derivative approximations, such as a four-point or eight-point central difference quotients to further minimize truncation error.

The numerical evaluation of Δ_{BG} has several advantages over the semianalytic formulas using expansions such as Eq. (10).

(i) The numeric routine uses full two-loop RGEs including all third-generation Yukawa couplings [96] and one-loop threshold effects while semianalytic expansions use one-loop RGEs without threshold effects.

(ii) The semianalytic expansions were formulated to compute the Higgs potential at a scale

$$Q \sim m_Z,$$

whilst the numeric routine uses an optimized scale choice

$$Q^2 = m_{\tilde{t}_1} m_{\tilde{t}_2}.$$

This latter choice matches the higher scales for MSSM/SM decoupling that are expected from LHC data.

(iii) Usually the semianalytic expansions are computed for a particular $\tan\beta$ value while the numeric evaluation is valid for all $\tan\beta$.

To illustrate the comparison between the two methods, in Fig. 2(a) we compute the ratio

$$\Delta_{\mathrm{BG}}(\text{numerical})/\Delta_{\mathrm{BG}}(\text{semianalytic})$$

in the m_0 vs $m_{1/2}$ plane of the mSUGRA/CMSSM plane for $A_0 = 0$ and $\tan\beta = 10$ with $\mu > 0$. The blue region corresponds to a ratio ~ 0.5 while for small m_0 we find a ratio $\lesssim 1$. For large m_0 then we find a ratio $\gtrsim 1$ with the ratio reaching as high as ~ 2 near the lower focus-point region.

In Fig. 2(b) we again compute the ratio

$$\Delta_{\mathrm{BG}}(\text{numerical})/\Delta_{\mathrm{BG}}(\text{semianalytic})$$

in the m_0 vs $m_{1/2}$ plane of the mSUGRA/CMSSM, but now for $A_0 = -2m_0$ and $\tan\beta = 10$ with $\mu > 0$. The large value of A_0 here permits the Higgs mass to be within the allowed range of 125 ± 2 GeV. The broad orange and red regions throughout the rhs of the plane correspond to where the ratio is ~ 1. The largest discrepancy between the evaluation methods occurs on the lhs of the plane near the stau lightest supersymmetric particle (LSP) region, where

$$\Delta_{\mathrm{BG}}(\text{numerical}) \sim 0.6 \Delta_{\mathrm{BG}}(\text{semianalytic}).$$

Figure 2(c) instead shows the ratio comparing the numerical method to the semianalytic method in the m_0 vs $m_{1/2}$ plane of the NUHM2 model with $\mu = 200$ GeV, $m_A = 2$ TeV, and $A_0 = -1.6 m_0$. Again, the broad orange and red region on the rhs of this plane shows very good agreement between the two methods,

$$\Delta_{\mathrm{BG}}(\text{numerical}) \sim \Delta_{\mathrm{BG}}(\text{semianalytic}).$$

On the lhs above the CCB minima region, where $m_{1/2} > m_0$, the semianalytic method result becomes somewhat larger than the numerical method result, leading to a minimal ratio

$$\Delta_{\mathrm{BG}}(\text{numerical}) \sim 0.57 \Delta_{\mathrm{BG}}(\text{semianalytic}).$$

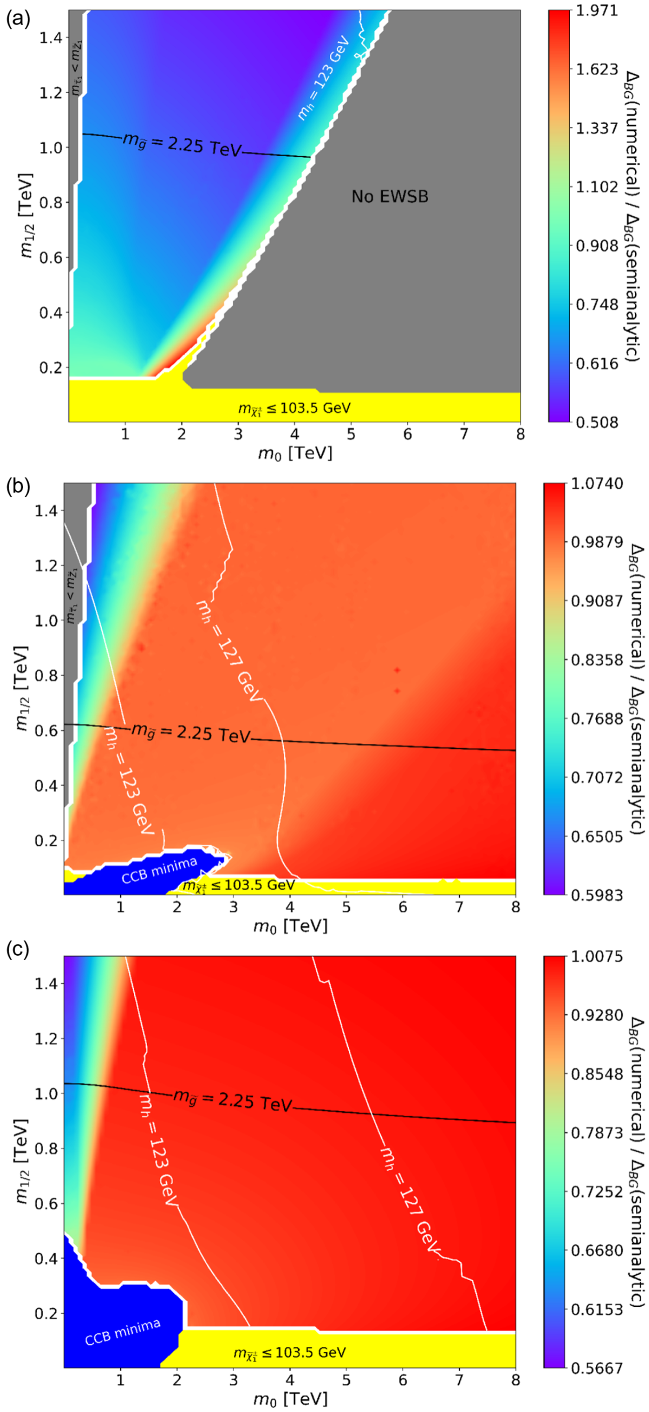

FIG. 2. Plot of $\Delta_{\rm BG}$(numerical)/$\Delta_{\rm BG}$(semianalytic) in the m_0 vs $m_{1/2}$ plane of (a) the CMSSM/mSUGRA model with $A_0 = 0$, $\tan\beta = 10$, and $\mu > 0$, (b) the CMSSM/mSUGRA model with $A_0 = -2m_0$, and (c) the NUHM2 model with $\mu = 200$ GeV and $A_0 = -1.6m_0$ with $m_A = 2$ TeV. We use the code DEW4SLHA to compute $\Delta_{\rm BG}$(numerical) using a numerical algorithm for the sensitivity coefficients and SOFTSUSY v4.1.17 for the spectra.

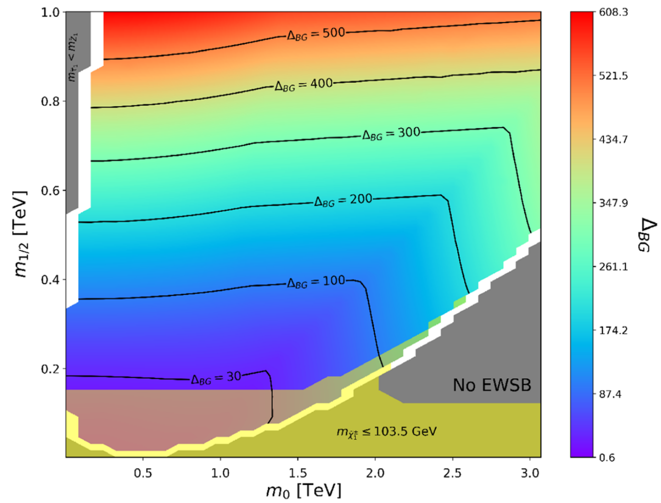

FIG. 3. Plot of naturalness contours $\Delta_{\rm BG}$ in the m_0 vs $m_{1/2}$ plane of the CMSSM/mSUGRA model with $A_0 = 0$, $\tan\beta = 10$, and $\mu > 0$. We use the code DEW4SLHA to compute $\Delta_{\rm BG}$ using a numerical algorithm for the sensitivity coefficients and SOFTSUSY for the spectra.

2. Numerical results for $\Delta_{\rm BG}$

In Fig. 3, we compute contours and color-coded regions of $\Delta_{\rm BG}$ in the mSUGRA/CMSSM model using a numerical routine to evaluate the sensitivity coefficients. This routine is embedded in the publicly available computer code DEW4SLHA. The results in Fig. 3 agree well with those presented by Allanach *et al.* in Ref. [97].

In truth, the various supposedly independent high-scale soft terms are introduced by hand in the mSUGRA/CMSSM model as a parametrization of our ignorance as to the SUSY-breaking mechanism. Indeed, in the case of gravity mediation, if we specify a specific SUSY-breaking mechanism, then all soft terms are calculable in terms of the gravitino mass $m_{3/2}$. An example is the famous dilaton-dominated SUSY-breaking model [68]; in this case

$$m_0 = m_{3/2} \quad \text{with} \quad m_{1/2} = -A_0 = \sqrt{3}m_{3/2}. \tag{12}$$

In such a case, then it doesn't make sense that the soft terms are independent; invoking PN, we should combine dependent terms in Eq. (10). Then,

$$m_Z^2 \simeq -2.18\mu^2 + 14.494m_{3/2}^2.$$

Adopting $m_{3/2} = 3$ TeV as in the previous example, then we find $\mu = 7735$ GeV and

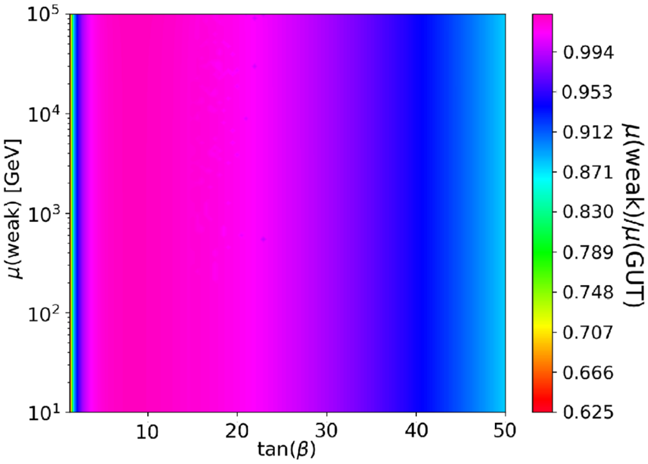

FIG. 4. Ratio of μ/μ_0 in the $\tan\beta$ vs μ(weak) plane, where $\mu_0 = \mu(\mathrm{GUT})$ is the GUT-scale value of the μ parameter.

$$\Delta_{\rm BG} = c_{m_{3/2}^2} = 15683.$$

The SUSY μ parameter evolves very little from the GUT scale to the weak scale, due to the supersymmetric nonrenormalization theorems [98]. The ratio of $\mu(\mathrm{weak})/\mu(\mathrm{GUT})$ is shown in Fig. 4 for the $\tan\beta$ vs μ(weak) plane in the mSUGRA/CMSSM model. The deviation between $\mu(\mathrm{weak})/\mu(\mathrm{GUT})$ is typically a few percent, climbing to $\sim$10% at very large $\tan\beta$.

Now, in the case where all soft terms are determined in terms of $m_{3/2}$ (such as gravity mediation, anomaly mediation and mirage mediation), then we expect roughly that

$$m_Z^2 \simeq -2\mu^2 + a \cdot m_{3/2}^2 \tag{13}$$

and since μ hardly evolves, then

$$a \cdot m_{3/2}^2 \simeq -2m_{H_u}^2(\mathrm{weak}).$$

In this case—with all correlated soft terms (which we may dub as the SUGRA1 model)—then

$$\Delta_{\rm BG} \sim c_{m_{3/2}^2} = a\frac{m_{3/2}^2}{m_Z^2} \simeq \frac{\max\left[2\mu^2, 2m_{H_u}^2(\mathrm{weak})\right]}{m_Z^2}.$$

This latter case we will find is nearly the same as $\Delta_{\rm EW}$ aside from the inclusion of the radiative corrections to the weak-scale scalar potential.

In Fig. 5, we plot naturalness contours in the same parameter plane as in Fig. 3, but now assuming instead the one-soft-parameter SUGRA1 model. For SUGRA1, we have

$$m_Z^2 = -2.18\mu_0^2 + a \cdot m_0^2 \quad (\mathrm{SUGRA1}), \tag{14}$$

where the constant a can be determined via

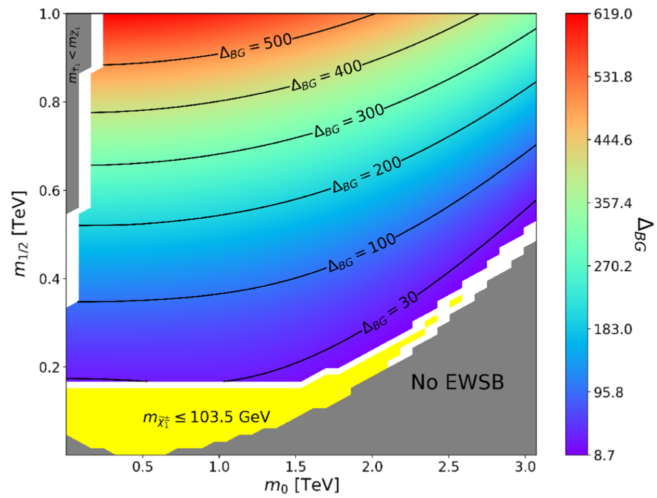

FIG. 5. Plot of naturalness contours $\Delta_{\rm BG}$ in the m_0 vs $m_{1/2}$ plane of the one-soft-parameter SUGRA1 model with $A_0 = 0$, $\tan\beta = 10$ and $\mu > 0$. We use SOFTSUSY to generate the spectra.

$$a = (m_Z^2 + 2.18\mu_0^2)/m_0^2.$$

In this case, the naturalness contours roughly follow the contours of constant μ value. For the case of SUGRA1, the naturalness contours are very different from the case of independent high-scale soft terms assumed in the mSUGRA/CMSSM model.

One may also define a SUGRA2 model. Here, we assume that since gaugino masses arise from the gauge kinetic function, this soft term is independent of the others which are determined instead by the Kähler function, but where A_0 is determined in terms of m_0 (such as $A_0 = -2m_0$) so that

$$m_Z^2 = -2.18\mu_0^2 + 3.786m_{1/2}^2 - 0.427m_0^2 + 1.642m_{1/2}m_0 \quad (\mathrm{SUGRA2}). \tag{15}$$

Finally, SUGRA3 allows that A_0 is somehow independent from m_0 (or $m_{3/2}$) so that

$$m_Z^2 = -2.18\mu_0^2 + 3.786m_{1/2}^2 + 0.013m_0^2 + 1.642m_{1/2}m_0 + 0.22A_0^2 \quad (\mathrm{SUGRA3}). \tag{16}$$

For the three cases, we find that the $\Delta_{\rm BG}$ values are very different in the SUGRA1, SUGRA2, or SUGRA3 models just depending on which parameters are assumed to be truly independent.

In Fig. 6, we show color-coded regions of $\Delta_{\rm BG}$ as computed in the m_0 vs $m_{1/2}$ plane of the NUHM2 model where $\tan\beta = 10$, $A_0 = -1.6m_0$, with $\mu = 200$ GeV and $m_A = 2$ TeV. In frame (a), we assume all soft terms are correlated as in Eq. (14). In this case, since μ is fixed, there is a constant value of $\Delta_{\rm BG} = 21.2$ throughout the plane.

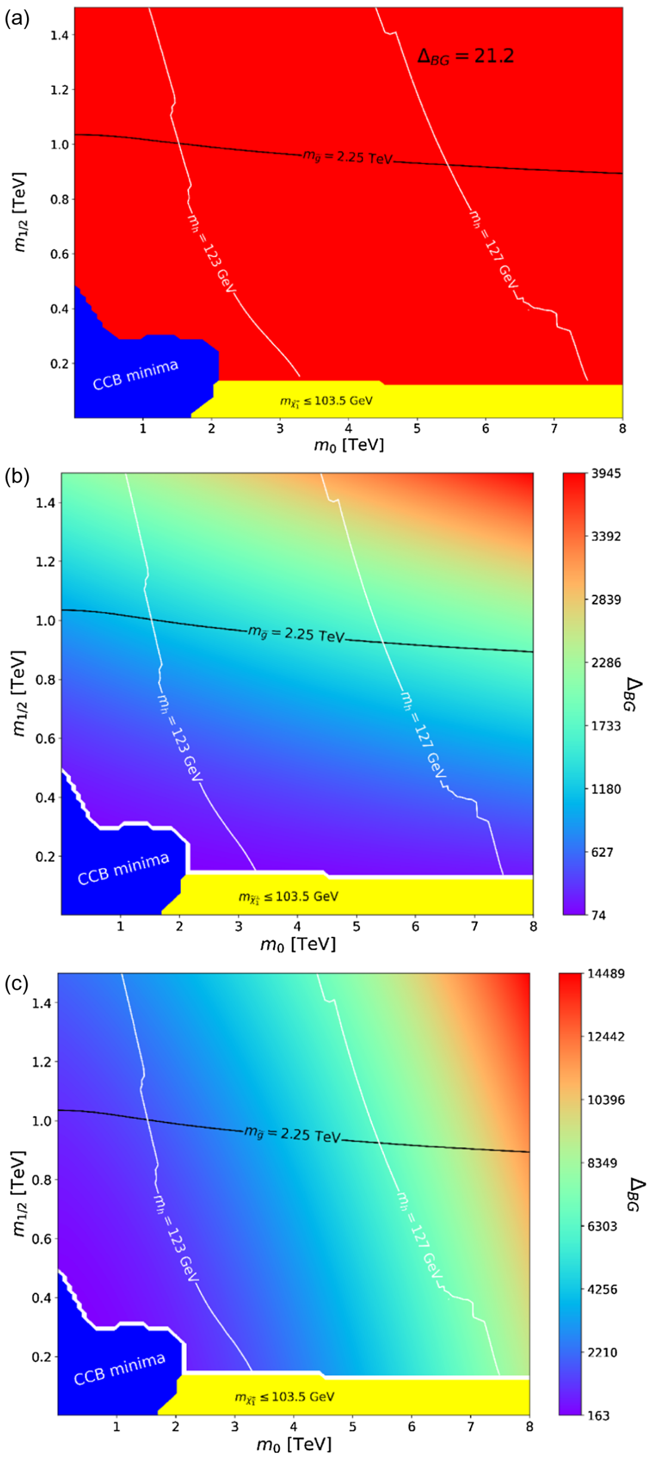

FIG. 6. Plot of $\Delta_{\rm BG}$ values in the m_0 vs $m_{1/2}$ plane for the NUHM2 model for $A_0 = -1.6m_0$, $\tan\beta = 10$ with $\mu = 200$ GeV and $m_A = 2$ TeV. In (a), we plot $\Delta_{\rm BG}$ assuming a single independent soft parameter $m_{3/2}$ while in (b) we plot $\Delta_{\rm BG}$ for assumed two independent soft parameters m_0 and $m_{1/2}$ while in (c) we plot assuming all three of m_0, $m_{1/2}$, and A_0 are independent. The spectra are calculated using SOFTSUSY and the naturalness measures with DEW4SLHA.

In frame 6(b), we instead assume two independent soft parameters m_0 and $m_{1/2}$ (but with A_0 fixed in terms of m_0) so that we are in the SUGRA2 model; Eq. (15). Here, the value of $\Delta_{\rm BG}$ is vastly different from frame 6(a), reaching up to values of $\sim$3900 in the upper-right corner; a factor of $\sim$180 times greater than the frame 6(a) value. Here, the $\Delta_{\rm BG}$ fine-tuning is dominated by the $m_{1/2}$ value but not so much by m_0. In frame 6(c), instead we show values of $\Delta_{\rm BG}$ assuming three independent soft parameters as in Eq. (16). In this case, with A_0 fixed as $A_0 = -1.6m_0$ but nonetheless declared as independent, we see a greater dependence on m_0, so $\Delta_{\rm BG}$ increases as m_0 increases, mainly because A_0 increases with increasing m_0. Here, $\Delta_{\rm BG}$ reaches maximal values of $\sim$14500 in the upper-right corner, a factor $\sim$680 larger than the frame 6(a) value.

In summary, from the discussion of this section, we see that the measure $\Delta_{\rm BG}$ could be a legitimate fine-tuning measure if there could be consensus on what constitutes independent parameters of the model. The plots also illustrate the extreme model dependence of $\Delta_{\rm BG}$, where $\Delta_{\rm BG}$ can obtain values differing by several orders of magnitude depending on which parameters p_i are assumed fundamental or independent.

B. High-scale fine-tuning

An alternative to EENZ/BG naturalness which we label as HS fine-tuning emerged early on in the 21st century. It may have been intended originally as a figurative bullet-point indicator to argue for sparticle masses near the weak scale [46], but later was regarded as a viable measure of fine-tuning [47,50–52]. This measure seeks to apply PN to the Higgs-boson mass relation [see, e.g., Eq. (10) of [99]]

$$m_h^2 \simeq \mu^2 + m_{H_u}^2(\text{weak}) + \text{EW} + \text{mixing} \tag{17}$$

where the EW corrections and mixings are already $\lesssim m_h^2$. To apply high-scale fine-tuning, one must then break $m_{H_u}^2(\text{weak})$ into

$$m_{H_u}^2(\text{weak}) = m_{H_u}^2(m_{\rm GUT}) + \delta m_{H_u}^2$$

and require $\delta m_{H_u}^2 \lesssim m_h^2$. The full one-loop expression for $\delta m_{H_u}^2$ may be obtained by integrating its one-loop RGE from $m_{\rm GUT}$ to $m_{\rm weak}$,

$$\frac{dm_{H_u}^2}{dt} = \frac{2}{16\pi^2}\left(-\frac{3}{5}g_1^2M_1^2 - 3g_2^2M_2^2 + \frac{3}{10}g_1^2S + 3f_t^2X_t\right), \tag{18}$$

where $t = \log Q$,

$$S = m_{H_u}^2 - m_{H_d}^2 + \mathrm{Tr}\left[\mathbf{m}_Q^2 - \mathbf{m}_L^2 - 2\mathbf{m}_U^2 + \mathbf{m}_D^2 + \mathbf{m}_E^2\right],$$

and

$$X_t = m_{Q_3}^2 + m_{D_3}^2 + m_{H_u}^2 + A_t^2.$$

In the literature [50–52], to gain a simple expression, the terms with gauge couplings are ignored and X_t is approximated as

$$X_t \sim m_{Q_3}^2 + m_{D_3}^2 + A_t^2,$$

where $m_{Q_3}^2$, $m_{D_3}^2$, and A_t^2 here are GUT-scale values. Then a single step integration leads to

$$\delta m_{H_u}^2 \sim -\frac{3}{8\pi^2} f_t^2 (m_{Q_3}^2 + m_{U_3}^2 + A_t^2) \log(\Lambda/m_{\mathrm{weak}}), \quad (19)$$

where the high-scale Λ is usually assumed $\sim m_{\mathrm{GUT}}$. The Δ_{HS} measure famously promoted three light third-generation squarks below the 500 GeV scale [51], and motivated intensive searches by the LHC Collaborations to root out light top-squark signals.

In order to compare Δ_{HS} more appropriately with Δ_{BG} and Δ_{EW}, we slightly redefine Δ_{HS} in terms of $m_Z^2/2$ [100] where in this case we take

$$m_Z^2/2 = \frac{(m_{H_d}^2(\Lambda) + \delta m_{H_d}^2 + \Sigma_d^d) - (m_{H_u}^2(\Lambda) + \delta m_{H_u}^2 + \Sigma_u^u)\tan^2\beta}{\tan^2\beta - 1} - (\mu^2(\Lambda) + \delta\mu^2) \quad (20)$$

and Λ is some input high scale, perhaps m_P or m_{GUT}. Then

$$\Delta_{\mathrm{HS}} = \max|\text{largest term on rhs of Eq. (20)}|. \quad (21)$$

In this way, the three measures become equal in certain limiting cases.

The Δ_{HS} measure is problematic on several counts

(1) It violates the PN precept in that, in simplifying $\delta m_{H_u}^2$, all dependence on $m_{H_u}^2(\Lambda)$ is lost, which hides the fact that $\delta m_{H_u}^2$ is actually dependent on $m_{H_u}^2(\Lambda)$. In fact, the bigger the assumed value for $m_{H_u}^2(\Lambda)$, then the bigger is the canceling correction $\delta m_{H_u}^2$ [101]. This is shown in Fig. 7 where we show the exact two-loop value of $\delta m_{H_u}^2$ vs $m_{H_u}^2(\mathrm{GUT})$, where the clear dependence of $\delta m_{H_u}^2$ on $m_{H_u}^2(\mathrm{GUT})$ is shown. The plot also shows that the bigger $m_{H_u}(\mathrm{GUT})$ becomes, then the more EW-natural

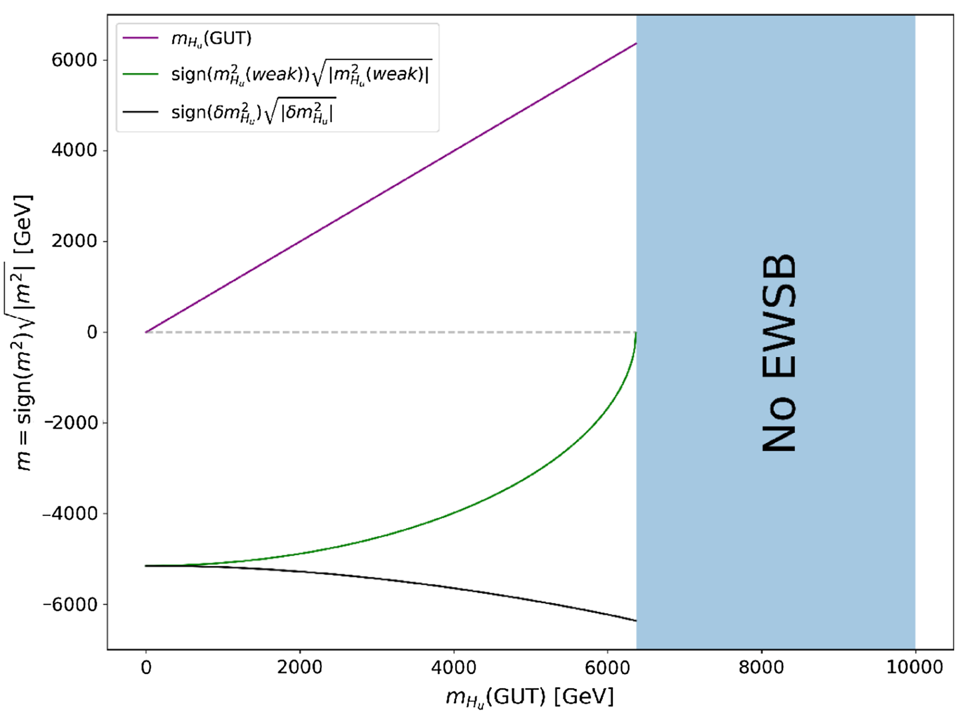

FIG. 7. Plot of $\mathrm{sign}(\delta m_{H_u}^2)\cdot\sqrt{|\delta m_{H_u}^2|}$ vs $m_{H_u}(\mathrm{GUT})$ for the NUHM2 model with $m_0 = 5$ TeV, $m_{1/2} = 1.2$ TeV, $A_0 = -1.6m_0$, $\tan\beta = 10$, and $m_{H_d} = 5$ TeV.

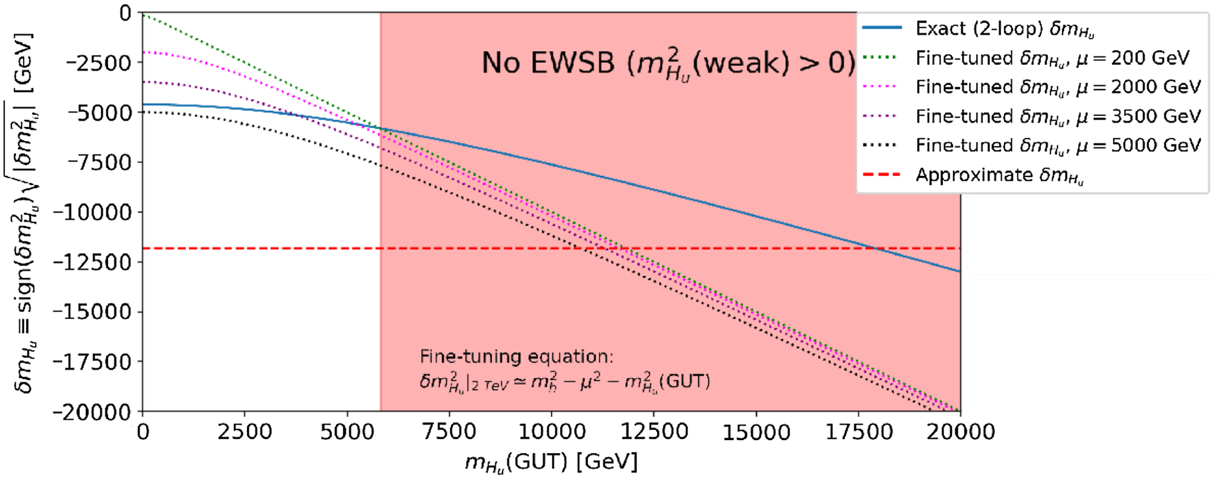

FIG. 8. Plot of $\mathrm{sign}(\delta m_{H_u}^2)\cdot\sqrt{|\delta m_{H_u}^2|}$ vs $m_{H_u}(\mathrm{GUT})$ for the NUHM2 model with $m_0 = 4.5$ TeV, $m_{1/2} = 1$ TeV, $A_0 = -7.2$ TeV, and $\tan\beta = 10$ with $m_A = 2$ TeV. We show the approximate expression Eq. (18) (red dashed curve) along with exact two-loop expression (blue solid) along with the value gleaned from fine-tuning for various values of μ.

the model becomes in that $m_{H_u}^2(\mathrm{weak})$ becomes comparable to m_Z^2 on the right-hand side shortly before EWSB is no longer broken. The splitting up of $m_{H_u}^2(\mathrm{weak})$ into $m_{H_u}^2(\Lambda) + \delta m_{H_u}^2$ turns Δ_{HS} into contradiction with Δ_{BG}, where $m_{H_u}^2(\mathrm{weak})$ is expanded into high-scale parameters in Eq. (10) but not split into $m_{H_u}^2(\Lambda) + \delta m_{H_u}^2$. This splitting of $m_{H_u}^2(\mathrm{weak})$ into dependent parts destroys the cancellations needed for focus point SUSY [40,41] which is promoted as allowing for TeV-scale top squarks.

(2) Electroweak symmetry breaking in SUSY models is accomplished by driving $m_{H_u}^2$ to negative values owing to the large top-quark Yukawa coupling f_t. Indeed, the REWSB mechanism is touted as one of the triumphs of WSS since it required $m_t \sim 100$–200 GeV [9] at a time when experiments seemed to indicate $m_t \sim 40$ GeV. By requiring $\delta m_{H_u}^2$ to be small, then often $m_{H_u}^2(\mathrm{weak})$ will not be large and negative enough to cause EWSB. In the context of vacua selection in the string landscape, such models without EWSB would likely not lead to inhabitable universes and would be vetoed. This can be viewed as a selection mechanism to favor models with large enough $\delta m_{H_u}^2$ such that EW symmetry is properly broken (see, e.g., Fig. 3 of Ref. [102].)

(3) There is also substantial ambiguity in evaluating Δ_{HS}. In Fig. 8 we show the value of

$$\delta m_{H_u} \equiv \mathrm{sign}\left(\delta m_{H_u}^2\right)\sqrt{\left|\delta m_{H_u}^2\right|}\ \mathrm{vs}\ m_{H_u}(\mathrm{GUT})$$

for an NUHM2 benchmark point with $m_0 = 4.5$ TeV, $m_{1/2} = 1$ TeV, and $A_0 = -7.2$ TeV with $\tan\beta = 10$ and $m_A = 2$ TeV. The approximate expression Eq. (19) is shown as the flat red-dashed line which of course does not depend on $m_{H_u}^2(\mathrm{GUT})$. The solid blue curve is the exact two-loop RG expression for δm_{H_u} and is shown to deviate from the approximate result by well over a factor of 2 at low $m_{H_u}(\mathrm{GUT})$ and only agrees with the approximation far into the excluded region where the electroweak symmetry is not properly broken. Alternatively, one may use the

$$m_h^2 \simeq \mu^2 + m_{H_u}^2 + \delta m_{H_u}^2$$

equation for a particular set of input parameters including $m_{H_u}^2(\mathrm{GUT})$ (e.g., in the NUHM2 model) to compute the value of $\delta m_{H_u}^2$ and then try to fine-tune $m_{H_u}^2(\mathrm{GUT})$ to enforce $m_h = 125$ GeV. But as one tunes the value of $m_{H_u}^2(\mathrm{GUT})$, then the value of $\delta m_{H_u}^2$ changes accordingly (as indicated by the various dotted lines for different input μ values), so that instead of finetuning, one must adopt an iterative procedure to try and find a solution. Sometimes the solution will migrate into the no EWSB region while other times the iterations can find a viable solution.

C. Electroweak naturalness

As mentioned before, the electroweak naturalness measure Δ_{EW} measures the largest contribution on the right-hand side of Eq. (3) and compares that to $m_Z^2/2$. This is the most conservative, unavoidable measure of naturalness since it is independent of any high-scale model. Even when high-scale parameters are correlated in some way, those correlations are typically lost under RG running and subsequent computation of the physical sparticle mass eigenstates. The interpretation of $\Delta_{\rm EW}$ is clear; if any one of the rhs contributions to Eq. (3) is far larger than $m_Z^2/2$, then it is highly implausible (but not impossible) that some other contribution would accidentally be large and of the opposite sign such that the two conspire to give an m_Z value of just 91.2 GeV. In this sense, natural models correspond to plausible models; models with large $\Delta_{\rm EW}$ are logically possible, but highly implausible. We will see later that this manifests itself as a probability, or likelihood, to emerge from scans over the string landscape.

The tree-level contributions to $\Delta_{\rm EW}$ are instructive:

(i) The SUSY conserving μ parameter, which sets the mass scale for the W, Z, h, and higgsinos enters the weak scale directly. We already know that $m_{W,Z,h} \sim 100$ GeV; the higgsinos should lie within a factor of several of the measured value of the weak scale. In light of LHC constraints, the SUSY LSP is likely a higgsinolike lightest neutralino, or at worst a gaugino-higgsino admixture.[7]

(ii) The value of $m_{H_u}^2$, where H_u acts as the SM Higgs doublet, should be driven to small, negative values since it also sets the mass of the W, Z, and h bosons.

(iii) The value of m_{H_d}, which sets the mass scale for the heavier Higgs bosons A, H and $H^\pm$, can be much larger since its contribution to the weak scale is suppressed by a factor of $\tan\beta$.

The loop-level contributions Σ_u^u and Σ_d^d are proportional to the individual particle/sparticle masses but since the Σ_d^d terms are suppressed by $\tan\beta$, the Σ_u^u terms are usually dominant. Of the Σ_u^u terms, usually $\Sigma_u^u(\tilde t_{1,2})$ are largest owing to the large top-quark Yukawa coupling. Since these terms are all suppressed by loop factors, the particle/sparticle masses which enter the Σ_u^u terms can be at the TeV or beyond scale before becoming comparable to the weak scale. Explicit expressions for the Σ_u^u and Σ_d^d are given in the Appendixes to Refs. [107] and [54]. The dominant terms are given by

$$\Sigma_u^u(\tilde t_{1,2}) = \frac{3}{16\pi^2} F(m_{\tilde t_{1,2}}^2) \times \left[f_t^2 - g_Z^2 \mp \frac{f_t^2 A_t^2 - 8 g_Z^2 (\frac{1}{4} - \frac{2}{3} x_W) \Delta_t}{m_{\tilde t_2}^2 - m_{\tilde t_1}^2} \right], \qquad (22)$$

where

$$F(m^2) = m^2 \left(\log \frac{m^2}{Q^2} - 1 \right)$$

and the optimized scale choice is taken as

$$Q^2 = m_{\tilde t_1} m_{\tilde t_2}.$$

Also,

$$\Delta_t = \frac{m_{\tilde t_L}^2 - m_{\tilde t_R}^2}{2} + m_Z^2 \cos(2\beta) \left(\frac{1}{4} - \frac{2}{3} x_W \right)$$

with

$$g_Z^2 = \frac{g^2 + g'^2}{8} \quad \text{and} \quad x_W = \sin^2\theta_W.$$

In the denominator of Eq. (22), the tree-level masses should be used.

Some highlights of the Σ_u^u terms include the following:

(i) For $\Delta_{\rm EW} \lesssim 30$, the top-squark contributions $\Sigma_u^u(\tilde t_{1,2})$ allow for top-squarks up to $m_{\tilde t_1} \lesssim 3$ TeV and $m_{\tilde t_2} \lesssim 8$ TeV. The explicit expressions contain large cancellations for large A_t both for $\Sigma_u^u(\tilde t_1)$ and $\Sigma_u^u(\tilde t_2)$. The large A_t helps to lift m_h into the 125 GeV range since m_h is maximal for $x_t \sim \sqrt{6} m_{\tilde t}$ [10]. This is in contrast to $\Delta_{\rm BG}$ and $\Delta_{\rm HS}$ which both prefer small trilinear soft terms. In Fig. 9 we show color-coded regions of $\Delta_{\rm BG}$ in the $m_{1/2}$ vs A_0 plane of the mSUGRA/CMSSM model for $m_0 = 5$ TeV, $\tan\beta = 10$ and $\mu > 0$. We also show contours of Higgs mass $m_h = 123$ GeV and 127 GeV, and contours of $\Delta_{\rm EW}$ and $\Delta_{\rm HS}$. The gray region around $A_0 \sim 0$ is the focus point region. From the plot, we see that $\Delta_{\rm HS}$ is always large, $\Delta_{\rm HS} \gtrsim 6000$, due to the large value of m_0. Meanwhile, $\Delta_{\rm BG}$ reaches as low as $\sim$1000, also in the FP region. $\Delta_{\rm EW}$ can reach as low as 62 in

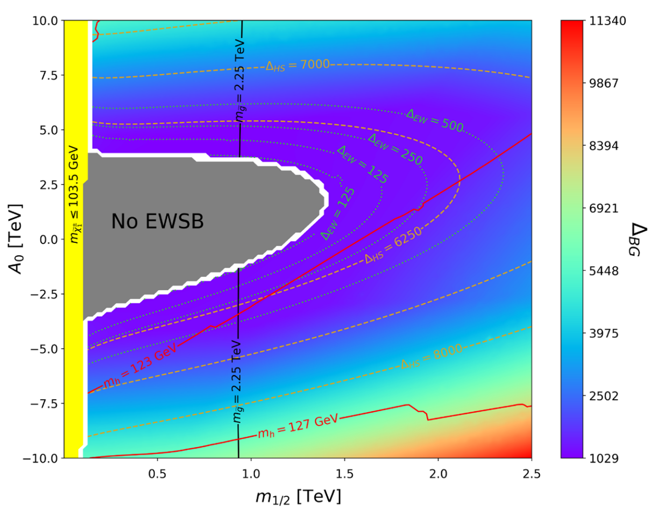

FIG. 9. Plot of color-coded values of $\Delta_{\rm BG}$ in the $m_{1/2}$ vs A_0 plane of the mSUGRA/CMSSM model for $m_0 = 5$ TeV, $\tan\beta = 10$, and $\mu > 0$. We also show contours of Higgs mass $m_h = 123$ GeV and 127 GeV, and contours of $\Delta_{\rm EW}$ and $\Delta_{\rm HS}$.

[7]We do not implement here constraints on SUSY models from the thermally produced neutralino relic density. The reason is that these bounds are easily superceded by nonthermal processes [103] such as axion-axino-saxion production [104] and/or the presence of moduli fields [105] in the early Universe. In such cases, the bulk of dark matter in SUSY models may indeed be axions [106].

between the two $\Delta_{\rm EW} = 125$ contours. As expected from the mSUGRA/CMSSM model, no points allow for both low fine-tuning and $m_h \sim 125$ GeV.

(ii) Since first-/second-generation Yukawa couplings are tiny, then these sparticle masses can be much larger than the third generation, with first-/second-generation squarks and sleptons ranging up to 30–50 TeV. In the context of the string landscape, this leads to a quasidegeneracy/decoupling solution to the SUSY-flavor and CP problems [78].

(iii) Gluinos affect the Σ_u^u via RG running and directly at the two-loop level [108]. They can range up to $m_{\tilde g} \lesssim 6$ TeV for $\Delta_{\rm EW} \lesssim 30$, well-beyond present LHC bounds [109].

A positive feature of $\Delta_{\rm EW}$ is its model independence (within the context of models for which the MSSM is the weak-scale EFT). The amount of fine-tuning only depends on the weak-scale spectrum which is generated, but not on how it is obtained. Thus, if one generates a certain weak-scale spectrum via some high-scale model, or just the pMSSM,[8] then one gets the same value of $\Delta_{\rm EW}$. This of course is not true for the measures $\Delta_{\rm HS}$ or $\Delta_{\rm BG}$.

A common criticism of $\Delta_{\rm EW}$ is that it doesn't account for high-scale parameter choices and correlations. This is not exactly true as discussed earlier. The μ parameter evolves only slightly from $m_{\rm GUT}$ to $m_{\rm weak}$, as shown in Fig. 4. With $\mu(m_{\rm GUT}) \simeq \mu(m_{\rm weak})$, and in the context of all soft terms correlated (as should be the case in a well specified SUSY-breaking model), then $\Delta_{\rm BG} \simeq \Delta_{\rm EW}$, sans the radiative corrections Σ_u^u and Σ_d^d. Also, if the dependent terms $m_{H_u}^2(\Lambda)$ and $\delta m_{H_u}^2$ are combined, as required by PN, then $\Delta_{\rm HS} \simeq \Delta_{\rm EW}$, without radiative corrections. Furthermore, the specific choices of high-scale parameters can lead to more or less fine-tuning via Eq. (3). In fact, a string landscape selection for larger soft terms often results in smaller values of $\Delta_{\rm EW}$ as compared to any selection for small or weak-scale soft terms [112].

D. Stringy naturalness: Anthropic origin of the weak scale

A fourth entry into the naturalness debate comes from Douglas [113] with regards to the string landscape; stringy naturalness, as remarked above. An advantage of stringy naturalness is that it actually provides an explanation for the magnitude of the weak scale, and not just naturalness of the weak scale. The distribution of vacua in the multiverse as a function of $m_{\rm soft}$ is expected to be

$$dN_{\rm vac} \sim f_{\rm SUSY}(m_{\rm soft}) \cdot f_{\rm EWSB}(m_{\rm soft}) dm_{\rm soft}. \qquad (23)$$

[8]For scans of $\Delta_{\rm EW}$ within the pMSSM, see, e.g., Refs. [110,111].

Douglas [113] advocates for a power-law draw to large soft terms based on the supposition that there is no favored value for SUSY-breaking fields on the landscape; $f_{\rm SUSY} \sim m_{\rm soft}^{2n_F+n_D-1}$ where n_F is the number of (complex-valued) F-breaking fields and n_D is the number of (real-valued) D-breaking fields giving rise to the ultimate SUSY-breaking scale. The distribution $f_{\rm EWSB}$ is suggested as $f_{\rm EWSB} = \Theta(30 - \Delta_{\rm EW})$ [114] such that the value of the weak scale in each pocket universe lies within the Agrawal-Barr-Donoghue-Seckel (ABDS) window [57], the so-called atomic principle. At present, SN does not admit a clear numerical measure [58].

V. COMPARISON OF MEASURES

From the previous discussion, it becomes clear that the various naturalness measures are defined very differently and hence we expect them to favor different regions of model parameter space. A figurative view of how the different measures compare can be gleaned from Fig. 10, which plots the evolution of the soft Higgs mass-squared parameter from $Q = m_{\rm GUT}$ to $Q = m_{\rm weak}$ in the NUHM2 model for $m_0 = 4.5$ TeV, $m_{1/2} = 1$ TeV, $A_0 = -1.6 m_0$, $\tan\beta = 10$, and $m_A = 2$ TeV. The right-side brackets correspond roughly to the different naturalness measures. In NUHM2, the BG measure contains a sensitivity coefficient

$$c_{m_{H_u}^2} \sim 1.27 |m_{H_u}(\Lambda)/m_Z|^2,$$

or

$$c_{m_{H_u}} \sim 2.54 |m_{H_u}(\Lambda)/m_Z|^2$$

if $m_{H_u}(\Lambda)$ is the fundamental parameter, instead of $m_{H_u}^2(\Lambda)$. Where this coefficient is the maximal contribution to $\Delta_{\rm BG}$, then this "distance" is the approximate measure. For $\Delta_{\rm HS} \simeq \delta m_{H_u}^2/m_Z^2$, the relevant measure is instead the bracketed distance $\delta m_{H_u}^2$, and so $\Delta_{\rm HS}$ is usually (but not always) larger than $\Delta_{\rm BG}$, since in order for EW symmetry to break, $m_{H_u}^2$ must be driven to negative values. Notice then from the plot that the only way for $\delta m_{H_u}^2$ to be small is also if $m_{H_u}^2(\Lambda)$ is small: this is why $\Delta_{\rm HS}$ favors only the low m_0 region when mSUGRA/CMSSM universality with $m_{H_u} = m_0$ is required. In contrast, low values of $\Delta_{\rm EW}$ require low $m_{H_u}^2$(weak), and so low $\Delta_{\rm EW}$ can be found for any value of $m_{H_u}^2(\Lambda)$ such that $m_{H_u}^2$ is barely driven to negative values. This is some times called criticality [102,115], or barely broken electroweak symmetry [116]. This latter quality is favored by the string landscape where as large as possible values of $m_{H_u}^2(\Lambda)$ are statistically favored so long as m_{Hu}^2 is just barely driven to negative values [114].

In Fig. 11(a), we plot naturalness favored and unfavored regions of parameter space in the mSUGRA/CMSSM model m_0 vs $m_{1/2}$ plane where $\tan\beta = 10$, $\mu > 0$ and

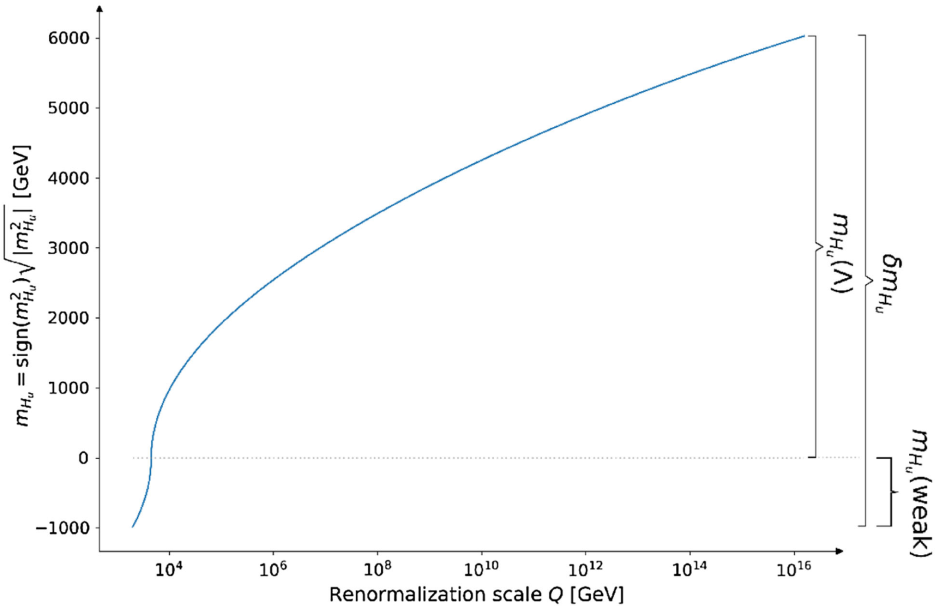

FIG. 10. Evolution of the $m^2_{H_u}$ soft SUSY breaking up-Higgs mass from $Q = m_{\mathrm{GUT}}$ to $Q = m_{\mathrm{weak}}$ for the NUHM2 model with $m_0 = 4.5$ TeV, $m_{1/2} = 1$ TeV, $A_0 = -1.6m_0$, $\tan\beta = 10$, and $m_A = 2$ TeV.

$A_0 = 0$ (spectra generated using SOFTSUSY [117]). The latter choice for A_0 is traditional in that it displays the FP region, which otherwise disappears for large A_0. However, it should be remarked here that $A_0 = 0$ is probably the least motivated value for A_0 in that in generic SUGRA models all soft terms are expected to occur of order $m_{3/2}$ and $m_{3/2} \sim m_0$. On the phenomenological side, small A_t leads to a near minimum in the Higgs mass m_h (as shown in Fig. 12) whilst $A_t \sim \sqrt{6}m_0$ leads to maximal m_h values [10]. Using high-scale parameters A_0, the range of A_t doesn't extend to the m_h maximal value before CCB minima are encountered in the scalar potential (which forms the endpoints of the plot). Currently, the mSUGRA/CMSSM FP region seems excluded by

(1) Too low a value of m_h [100] and
(2) The LSP DM candidate is of the well-tempered [118,119] type which is now excluded [120–122] by weakly interacting massive particles spin-independent direct-detection experiments such as xenon [123] and LZ [124].

From Fig. 11(a), we see the Δ_{BG} contours of 30 and 100 roughly track lines of constant μ for lower m_0 values and lines of m_0 for high values [41]. Meanwhile, the contour $\Delta_{\mathrm{EW}} = 30$ (denoted as blue), follows the low μ values to

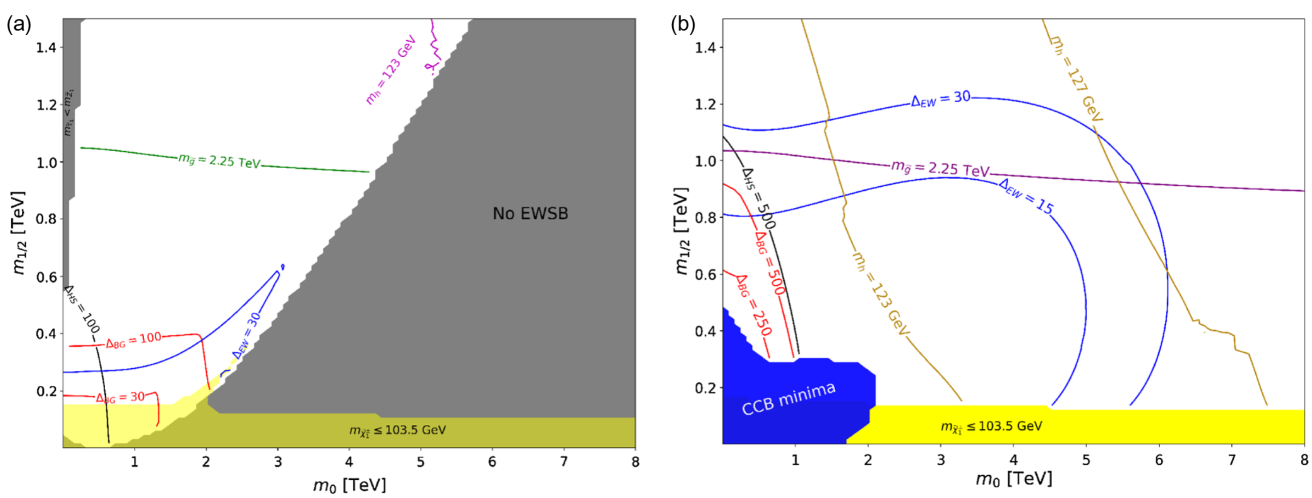

FIG. 11. Plot of various naturalness contours in (a) the mSUGRA/CMSSM m_0 vs $m_{1/2}$ plane for $A_0 = 0$ and $\tan\beta = 10$ and $\mu > 0$. In (b), we plot naturalness contours in the m_0 vs $m_{1/2}$ plane of the NUHM2 model with $A_0 = -1.6m_0$, $\tan\beta = 10$, $\mu = 200$ GeV and $m_A = 2$ TeV. The spectra are calculated using SOFTSUSY and the naturalness measures with DEW4SLHA.

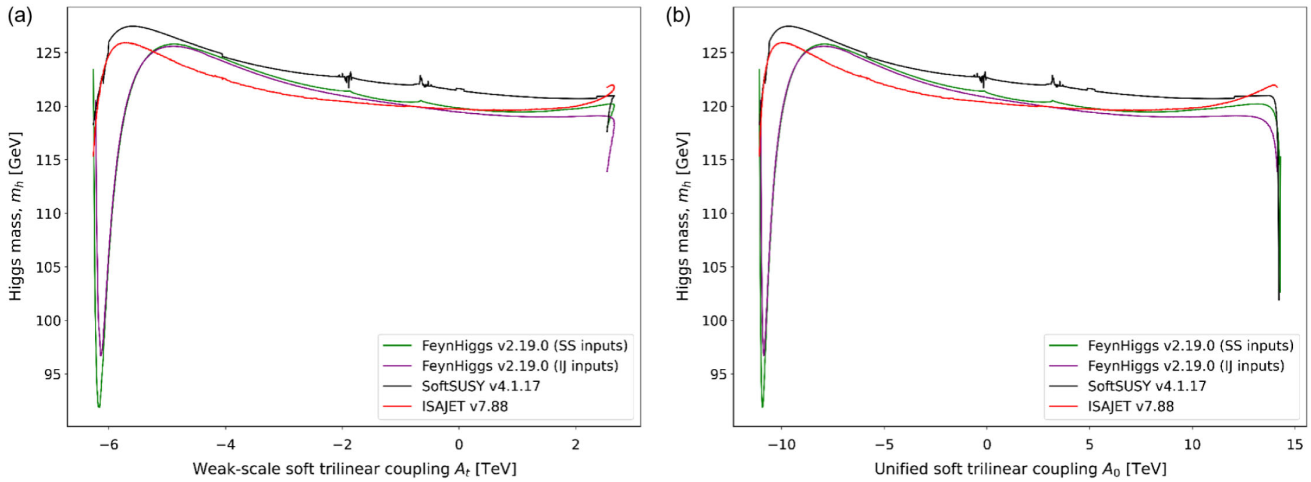

FIG. 12. Computed value of m_h vs (a) A_t and (b) A_0 in the mSUGRA/CMSSM model for $m_0 = 5$ TeV, $m_{1/2} = 1.2$ TeV and $\tan\beta = 10$, with $\mu > 0$. We compare the results from SOFTSUSY [117], FeynHiggs [125] using SOFTSUSY or ISAJET inputs, and ISASUGRA 7.88 [126].

much larger m_0 whereupon it cuts off due to increasing top-squark contributions via the $\Sigma_u^u(\tilde{t}_{1,2})$ terms. The conflict of these measures with $\Delta_{\rm HS}$ is apparent since $\Delta_{\rm HS}$ favors light third-generation squarks which occur only at low m_0 and low $m_{1/2}$. All three measures favor the lower corner of m_0 vs $m_{1/2}$ parameter space, and, when compared to LHC gluino mass limits ($m_{\tilde{g}} \gtrsim 2.25$ TeV as shown by the green contour), might lead one to conclude this model is excluded based on comparisons of naturalness with LHC constraints.

A very different picture emerges when one proceeds to the NUHM2 model as shown in Fig. 11(b). In this case, nonuniversality of the Higgs soft masses (as expected in gravity- mediation) allows for low $\mu = 200$ GeV throughout the parameter plane. Also, the large negative $A_0 = -1.6m_0$ term allows for $m_h \sim 125$ GeV throughout much of the plane (as shown between the gold contours of mass $m_h = 123$ GeV and 127 GeV). The large, negative A_0 term helps crunch the $\Delta_{\rm HS}$ and $\Delta_{\rm BG}$ contours into the lower-left region which actually yields charge-and-color breaking scalar potential minima, which must be excluded. Meanwhile, the $\Delta_{\rm EW}$ contours balloon out to very large m_0 and $m_{1/2}$ values, with $\Delta_{\rm EW} \sim 30$ extending well-beyond present LHC limits on $m_{\tilde{g}}$. While the lowest $\Delta_{\rm EW}$ values are still found in the lower-left corner of m_0 vs $m_{1/2}$ parameter space, we note that stringy naturalness, which favors a power-law draw to large soft terms, actually favors the region beyond the LHC $m_{\tilde{g}}$ limit [58].

VI. RATIOS OF MEASURES FOR CMSSM AND NUHM2 MODELS

In this section we compute the ratios of various naturalness measures in the CMSSM/mSUGRA and NUHM2 models. Spectra are calculated with SOFTSUSY [117] while naturalness measures are computed with DEW4SLHA [54]. The goal here is to quantify potential overestimates of finetuning in different SUSY models.

A. Ratios of measures for the mSUGRA/CMSSM model

1. Results in m_0 vs $m_{1/2}$ plane

In Fig. 13, we compute the various ratios of naturalness in the mSUGRA/CMSSM model and display results in the m_0 vs $m_{1/2}$ plane for $A_0 = 0$ and $\tan\beta = 10$, such as to include the HB/FP region. Our first results are shown in frame (a) where we plot $\Delta_{\rm HS}/\Delta_{\rm BG}$. The right-side gray region has no EWSB while the left-side gray region has a stau LSP. The lower-yellow region has the lightest chargino below LEP2 limits of $m_{\tilde{\chi}_1^\pm} < 103.5$ GeV. The color-coded ratios are denoted by the scale on the right-hand side of the plot and range from 0.5 (purple) to ∼15 (red).

Starting from the lhs of Fig. 13(a), we see that for low m_0 then $\Delta_{\rm HS} \sim \Delta_{\rm BG}/2$. This is because $\Delta_{\rm BG}$ is typically dominated by the gluino or M_3 contribution which is then canceled by μ^2 to maintain m_Z at 91.2 GeV. But $\Delta_{\rm HS}$ is dominated instead by $\delta m_{H_u}^2$ which is low at low m_0. As m_0 increases, then ultimately the two measures are comparable in the color transition region while for higher m_0 values, where the FP-type cancellation kicks in, then $\Delta_{\rm HS}$ becomes much larger than $\Delta_{\rm BG}$ and reaches nearly a factor of ∼5–15 at the edge of the "no EWSB" region. This plot illustrates that the $\Delta_{\rm BG}$ and $\Delta_{\rm HS}$ measures are incompatible.

In Fig. 13(b), we plot the ratio $\Delta_{\rm BG}/\Delta_{\rm EW}$. In this case, on the left side at low m_0 the two measures are comparable, but become as large as a factor ∼15 on the rhs near the edge of the *no EWSB* excluded region. In this region, $\Delta_{\rm BG}$ is dominated by the gluino/M_3 contribution, but in $\Delta_{\rm EW}$ this is two-loop suppressed and so $\Delta_{\rm BG}$ is much larger.

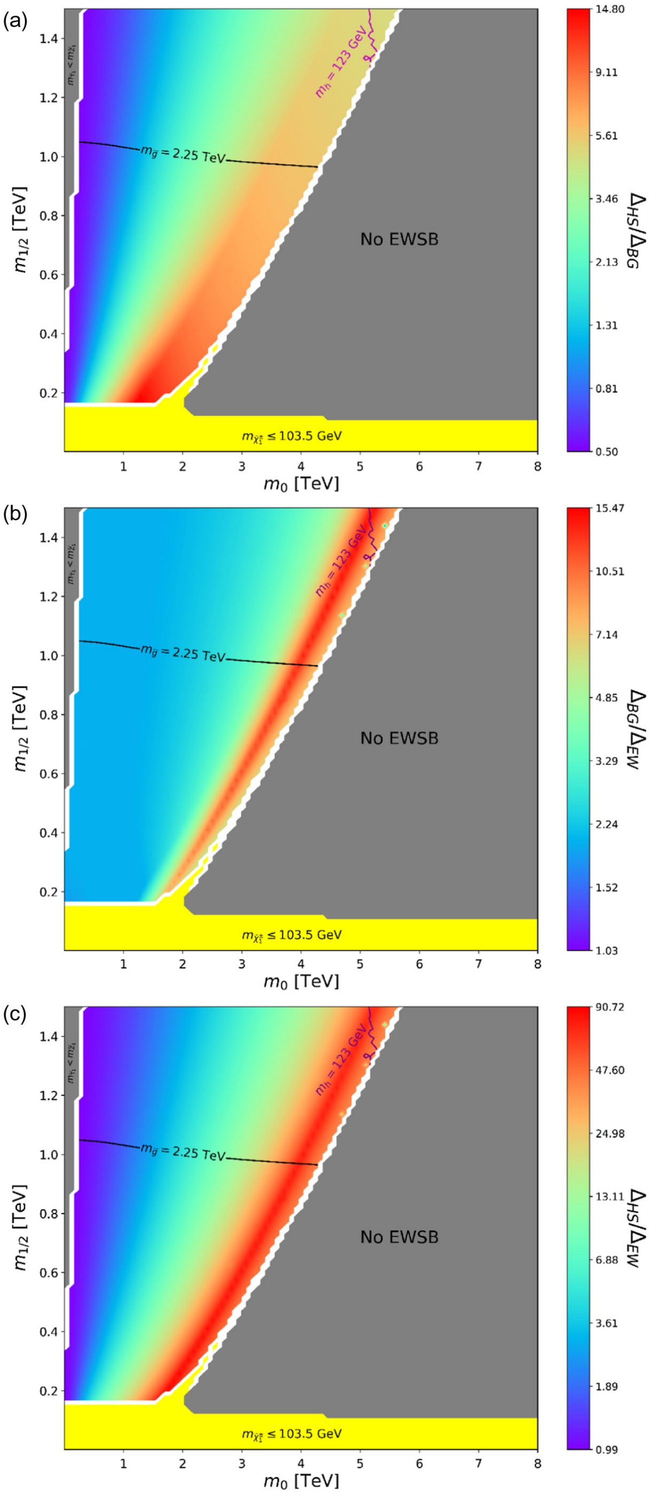

FIG. 13. Plot of ratios of naturalness measures in the m_0 vs $m_{1/2}$ plane for the CMSSM model for for $A_0 = 0$, $\tan\beta = 10$, and $\mu > 0$. In (a), we plot $\Delta_{\rm HS}/\Delta_{\rm BG}$ while in (b) we plot $\Delta_{\rm BG}/\Delta_{\rm EW}$ and in (c) we plot $\Delta_{\rm HS}/\Delta_{\rm EW}$. The spectra are calculated using SOFTSUSY and the naturalness measures with DEW4SLHA.

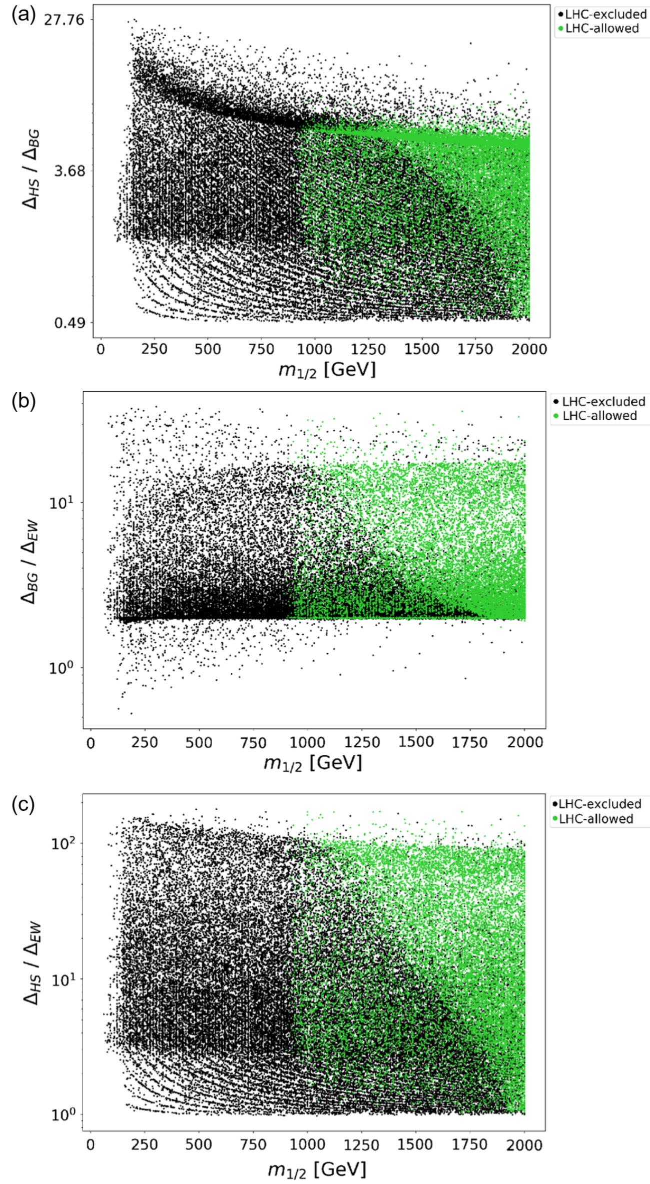

FIG. 14. Plot of ratios of naturalness measures vs $m_{1/2}$ from a scan over CMSSM model parameters. In (a), we plot $\Delta_{\rm HS}$ vs $\Delta_{\rm BG}$ for a general plus a focused scan (at $A_0 = 0$ to pick up the FP SUSY region) while in (b) we plot $\Delta_{\rm BG}/\Delta_{\rm EW}$ and in (c) we plot $\Delta_{\rm HS}/\Delta_{\rm EW}$. The spectra are calculated using SOFTSUSY and the naturalness measures with DEW4SLHA.

In Fig. 13(c), where the ratio $\Delta_{\rm HS}/\Delta_{\rm EW}$ is plotted, we see the measures are only comparable on the extreme LHS but then differ by up to a factor of ~80–100 on the rhs in the orange/red region. In this region, top-squarks are in the multi-TeV regime so $\Delta_{\rm HS}$ is very large while $\Delta_{\rm EW}$ allows for multi-TeV top squarks owing to the loop factor in Eq. (22).

2. Results from scan over CMSSM parameters

Next, we attempt to pick out the maximal ratio of naturalness measures in an attempt to quantify their numerical differences. First, we scan over CMSSM parameter space:

(i) m_0: 0.1–15 TeV,
(ii) $m_{1/2}$: 0.1–2 TeV,
(iii) A_0: $-2.5m_0$ to $+2.5m_0$,
(iv) $\tan\beta$: 3–60

with $\mu > 0$. In Fig. 14(a), we show the ratio $\Delta_{\rm HS}/\Delta_{\rm BG}$ from the above scan plus a focused scan over the same parameter range but with $A_0 = 0$ so as to pick up the FP region where the ratio is expected to be largest. The green points are LHC-allowed from LHC Run 2. In this case, the ratio $\Delta_{\rm HS}/\Delta_{\rm BG}$ can be as high as 28 overall, but only as high as $\sim$10 in the LHC-allowed region. These values are somewhat higher than the maximal ratios obtained from the plane plots.

Similarly, we show in Fig. 14(b) the ratio $\Delta_{\rm BG}/\Delta_{\rm EW}$ which ranges up to 50 (20) in the overall (LHC-allowed) case. In frame (c), the ratio $\Delta_{\rm HS}/\Delta_{\rm EW}$ ranges up to $\sim$200 for both LHC-allowed and forbidden cases.

B. Ratios of measures for the NUHM2 model

1. Results in m_0 vs $m_{1/2}$ plane

Next, we compute ratios of naturalness measures for the NUHM2 model. In this case, we expect much bigger differences between naturalness measures $\Delta_{\rm BG}$ and $\Delta_{\rm EW}$ since for NUHMi models, $m_{H_u}^2$ is now a free parameter, and no longer available to cancel against other oppositely signed sfermion contributions in Eq. (10). In particular, the FP cancellation between Higgs and third-generation sfermion terms in Eq. (10) is destroyed when one assumes that $m_{H_u}^2$ is a free parameter. Furthermore, by adopting natural values of $\mu \sim m_{\rm weak}$, then this contribution to $\Delta_{\rm EW}$ is suppressed and the dominant contribution instead frequently comes from the (loop-suppressed) $\Sigma_u^u(\tilde{t}_{1,2})$ terms.

In Fig. 15(a), we show color-coded ratios $\Delta_{\rm HS}/\Delta_{\rm BG}$ in the m_0 vs $m_{1/2}$ plane of the NUHM2 model with $A_0 = -1.6m_0$, $\tan\beta = 10$, $\mu = 200$ GeV, and $m_A = 2$ TeV. The lower-left blue-shaded region has CCB minima in the scalar potential owing in part to the large A_0 term. The mass spectra are generated using SOFTSUSY. The gold contours denote Higgs mass $m_h = 123$ GeV (left) and $m_h = 127$ GeV (right), while the purple contour near $m_{1/2} \sim 1$ TeV denotes the LHC $m_{\tilde{g}} = 2.25$ TeV limit. On the green-shaded extreme left side of the plot, $\Delta_{\rm BG}$ becomes larger than $\Delta_{\rm HS}$ by a factor $\sim$2. For the bulk of the plot range (red- and orange- shaded regions), then $\Delta_{\rm HS} \sim (0.75$–$0.85)\Delta_{\rm BG}$.

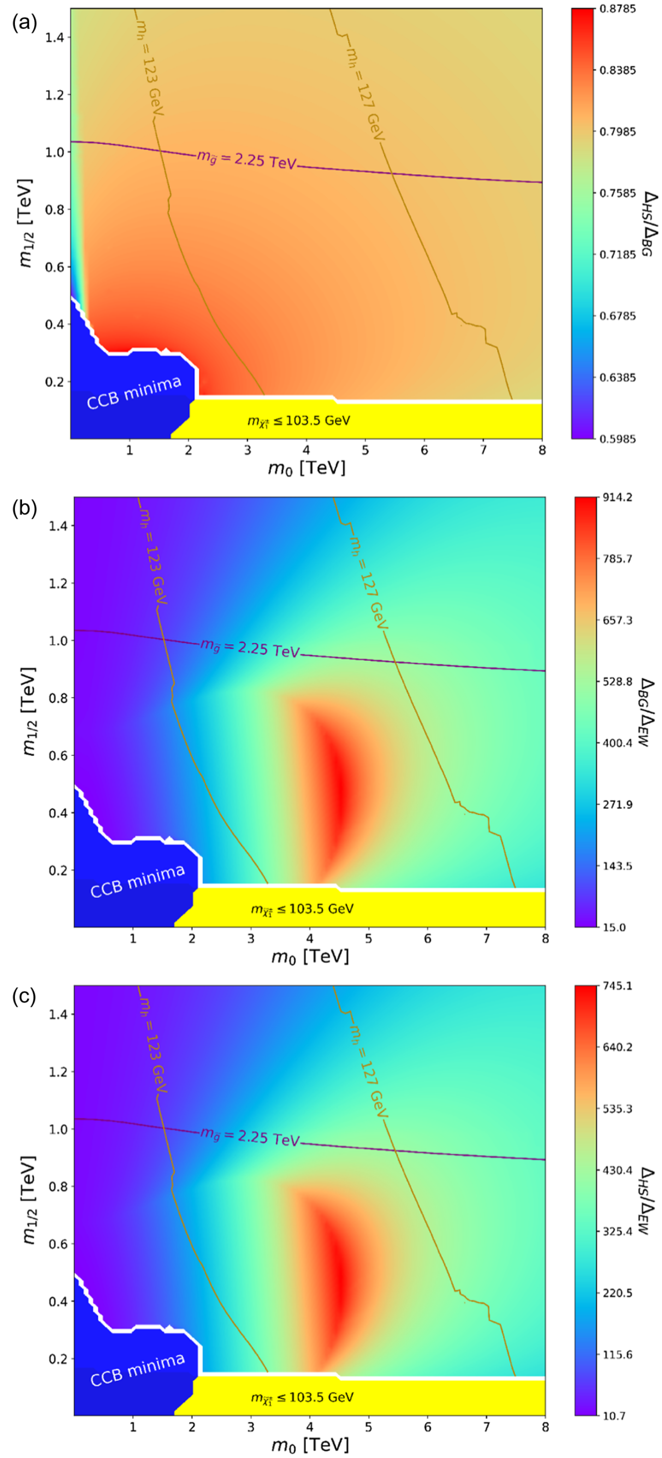

FIG. 15. Plot of ratios of naturalness measures in the m_0 vs $m_{1/2}$ plane for the NUHM2 model for $A_0 = -1.6m_0$, $\tan\beta = 10$ and $\mu = 200$ GeV, and $m_A = 2$ TeV. In (a), we plot $\Delta_{\rm BG}/\Delta_{\rm HS}$ while in (b) we plot $\Delta_{\rm BG}/\Delta_{\rm EW}$ and in (c) we plot $\Delta_{\rm HS}/\Delta_{\rm EW}$. The spectra are calculated using SOFTSUSY and the naturalness measures with DEW4SLHA.

In Fig. 15(b), we show the ratio $\Delta_{\mathrm{BG}}/\Delta_{\mathrm{EW}}$ in the same plane as frame (a). In the red-shaded region below the LHC gluino mass limit, we see that $\Delta_{\mathrm{BG}}/\Delta_{\mathrm{EW}} \sim 900$, a gross disparity between measures. Here, we have utilized m_{H_u} as the fundamental parameter in place of $m^2_{H_u}$ for numerical stability purposes, as the difference is only a factor of two in the derivative. In this region, Δ_{BG} is dominated by the term

$$\frac{|-1.27 \cdot 2m^2_{H_u}|}{m^2_Z/2}$$

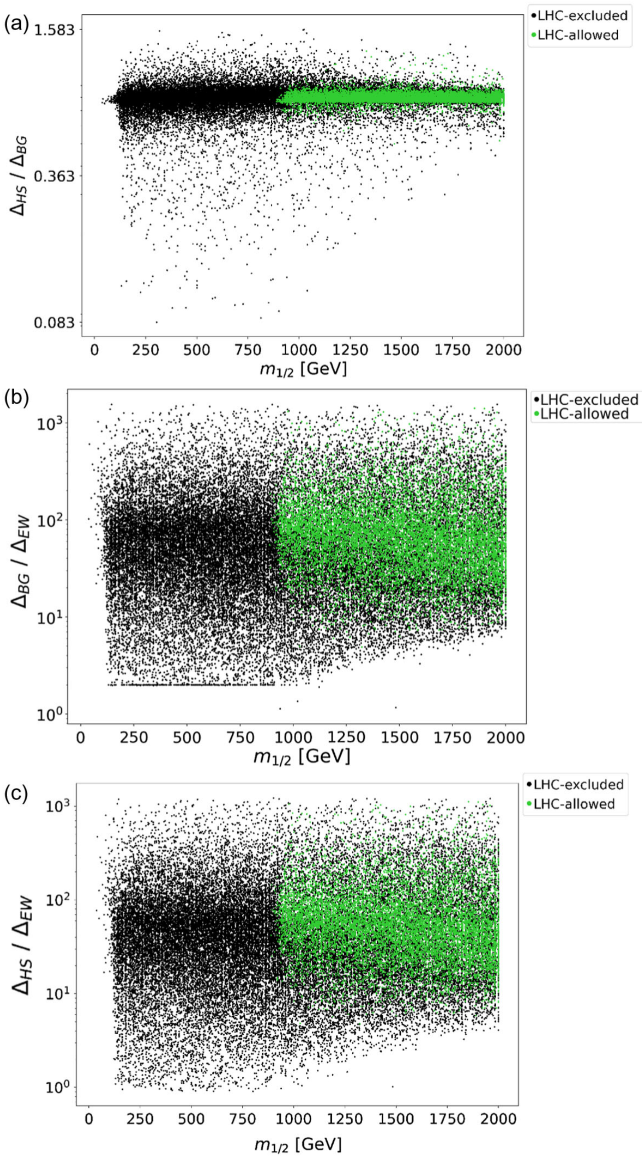

FIG. 16. Plot of ratios of naturalness measures vs $m_{1/2}$ from a scan over NUHM2 model parameters. In (a), we plot $\Delta_{\mathrm{HS}}/\Delta_{\mathrm{BG}}$ while in (b) we plot $\Delta_{\mathrm{BG}}/\Delta_{\mathrm{EW}}$, and in (c) we plot $\Delta_{\mathrm{HS}}/\Delta_{\mathrm{EW}}$. The spectrum is calculated using SOFTSUSY and the naturalness measures with DEW4SLHA.

in Eq. (10) which can be ~11000 whilst the Δ_{EW} measure is dominated by $\Sigma^u_u(\tilde{t}_{1,2})$ which yields $\Delta_{\mathrm{EW}} \sim 10$–20 (very natural). Throughout the NUHM2 plane, one can be brought to very different conclusions regarding the naturalness of the NUHM2 model parameter space depending on which measure one adopts. For the bulk of parameter space above the LHC gluino bound, then one finds $\Delta_{\mathrm{BG}} \sim (50\text{–}400)\Delta_{\mathrm{EW}}$.

In Fig. 15(c), we show the ratio $\Delta_{\mathrm{HS}}/\Delta_{\mathrm{EW}}$. In this case, the red-shaded region shows that $\Delta_{\mathrm{HS}} \sim 700\Delta_{\mathrm{EW}}$. Again, one is led to very different conclusions on the naturalness of the model depending on which measure one chooses. In this case, in the LHC-allowed region then $\Delta_{\mathrm{HS}} \sim (50\text{–}400)\Delta_{\mathrm{EW}}$.

2. Results from scan over NUHM2 parameters

Here, we scan over NUHM2 parameter space:

(i) m_0: 0.1–15 TeV,
(ii) $m_{1/2}$: 0.1–2 TeV,
(iii) A_0: $-2.5m_0$ to $+2.5m_0$,
(iv) $\tan\beta$: 3–60,
(v) μ: 0.1–1 TeV and
(vi) m_A: 0.3–8 TeV.

From Fig. 16(a), we see the ratio $\Delta_{\mathrm{HS}}/\Delta_{\mathrm{BG}}$ ranges from ~0.1–1.5 over the parameter space scanned: the two measures are rather close much of the time in this case, but sometimes Δ_{BG} can become a factor of ~10 larger than Δ_{HS}. In Fig. 16(b), instead we plot the $\Delta_{\mathrm{BG}}/\Delta_{\mathrm{EW}}$ ratio. While the bulk of parameter points have ratio between ~1–250, some few points can range up to 500–1000. Similar results are obtained for Fig. 16(c) where we plot $\Delta_{\mathrm{HS}}/\Delta_{\mathrm{EW}}$ and find ratios ranging again up to over 1000.

VII. NATURAL GENERALIZED ANOMALY MEDIATION (nAMSB)

Anomaly-mediated SUSY-breaking (AMSB) models [79,80] are good examples of models where the soft terms are all correlated and determined by a single parameter, the gravitino mass $m_{3/2}$. AMSB models assume a sequestering between the hidden and visible sector fields such that gravity-mediated soft terms are suppressed; in such a case, the loop-induced AMSB soft terms, which depend on the beta functions and anomalous dimensions of the low energy theory (assumed to be the MSSM) are dominant, and independent of higher-energy physics. At first glance, AMSB SUSY models would seem ruled out since the AMSB soft terms give rise to tachyonic sleptons. In the original Randall-Sundrum paper [79], it is conjectured that additional bulk soft terms may also be present which can solve the tachyonic slepton mass problem.

In the so-called minimal AMSB (mAMSB) model [127,128], a universal bulk sfermion mass m_0 is also assumed so that the parameter space of mAMSB is given by

$$m_0, m_{3/2}, \tan\beta, \mathrm{sign}(\mu) \quad (\mathrm{mAMSB}). \tag{24}$$

Here, the magnitude of a bilinear soft B term is traded for the parameter $\tan\beta$ and $|\mu|$ is determined from the EW minimization condition. Famously, the winolike neutralino turns out to be the LSP. At present, in light of LHC sparticle and Higgs mass constraints and direct/indirect wino dark matter constraints, mAMSB seems ruled out [120,129,130]. The small AMSB A_t terms lead to $m_h \ll 125$ GeV unless sparticle masses $\sim$10–100 TeV (highly unnatural) sparticle are assumed [131,132] and the DM constraints are evaded.

However, in Ref. [81] some minor fixes (already proposed in the original RS paper) were proposed which lead to generalized AMSB models (gAMSB) which allow for naturalness (nAMSB with $\Delta_{\mathrm{EW}} \lesssim 30$) and with $m_h \sim 125$ GeV. The fixes are:

(1) Nonuniversal scalar bulk masses $m_{H_u} \neq m_{H_d} \neq m_0$;
(2) Bulk-induced A_0 terms;
(3) A further option is independent bulk terms for each sfermion generation $m_0(i)$ with $i = 1$–3.

As in NUHMi models, the nonuniversal bulk Higgs soft terms can be traded for μ and m_A via scalar potential minimization conditions and the bulk A terms can be chosen to dial up $m_h \sim 125$ GeV. Thus, the generalized AMSB parameter space is given by

$$m_0(i), m_{3/2}, A_0, \tan\beta, \mu \quad \text{and} \quad m_A \quad (\text{gAMSB}). \tag{25}$$

For natural values of $\mu \sim 100$–350 GeV, then in the nAMSB model, the LSP is instead (usually) higgsinolike, although the wino is still the lightest of the gauginos. The gAMSB model is what one may expect in models of charged SUSY breaking, where the hidden sector SUSY breaking field S contains some hidden sector charge [133,134]. In this case, then usual gravity-mediated gaugino masses are forbidden since the gauge kinetic function is holomorphic. But sfermion masses and A-terms, which depend instead on the Kähler potential, are allowed to obtain gravity-mediated soft

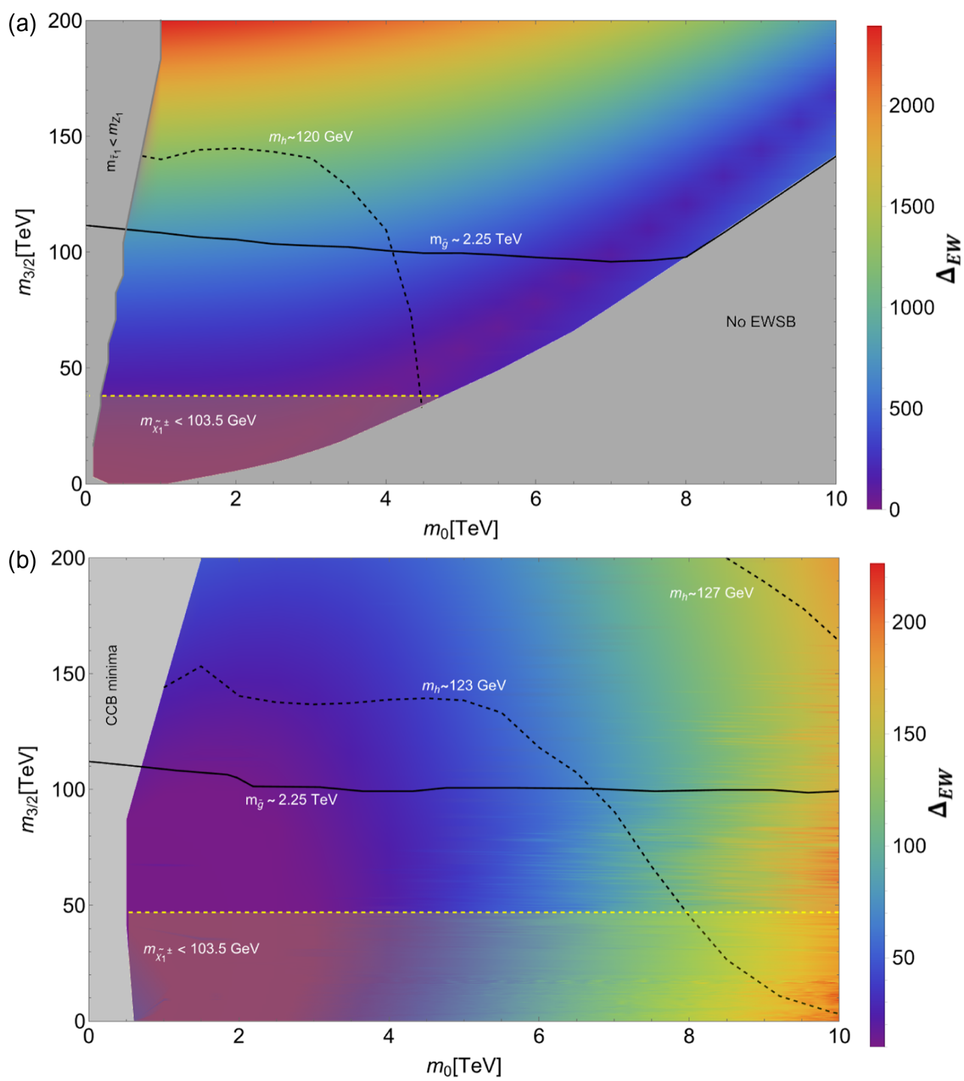

FIG. 17. Plot of naturalness measure Δ_{EW} in the m_0 vs $m_{3/2}$ plane of (a) the mAMSB model and (b) the nAMSB model for $\tan\beta = 10$. For nAMSB, we also require $\mu = 200$ GeV and $m_A = 2$ TeV. The spectra are calculated using Isasugra.

terms. The naturalness measure $\Delta_{\rm BG}$ is harder to interpret in the AMSB case since $m_{3/2}$ plays a more fundamental role than the *ad hoc* soft terms. Also, $\Delta_{\rm HS}$ is problematic in that the purely AMSB soft terms are famously scale independent, so there is no prescription for which Λ should be used in Eq. (19). Alternatively, there is no ambiguity in the $\Delta_{\rm EW}$ measure, so we proceed to exhibit its value.

In Fig. 17, we plot color-coded regions of the naturalness measure $\Delta_{\rm EW}$ in the m_0 vs $m_{3/2}$ plane for (a) the mAMSB model and (b) for the nAMSB model. For both cases, we take $\tan\beta = 10$ and $\mu > 0$. For the nAMSB model, we also take $\mu = 200$ GeV, $m_A = 2$ TeV and $A_0 = m_0$. In the case of frame (a) for the mAMSB model, the Higgs mass m_h is less then 123 GeV throughout the entire plane shown (and we do show a contour of $m_h = 120$ GeV via the dotted curve). The minimal value of $\Delta_{\rm EW}$ is ~25 in the purple focus point region of the LHC-excluded zone, but $\Delta_{\rm EW}$ can range as high as over 2000 in the upper-left region.

In contrast, for frame (b), we see that a large portion of the plane shown has $m_h \sim 123$–127 GeV. In addition, $\Delta_{\rm EW}$ can range as low as ~15 in the lower-left region, although this is excluded by LHC. In the LHC-allowed region, above the $m_{\tilde g} = 2.25$ TeV contour, then $\Delta_{\rm EW}$ can be as low as ~20. Note that the range of color-coded $\Delta_{\rm EW}$ values is much smaller in frame (b) than in (a); in (b), $\Delta_{\rm EW}$ ranges as high as ~150 while in (a) it can range beyond 2000.

VIII. NATURAL GENERAL MIRAGE MEDIATION

While the AMSB models may seem contrived owing to the requirement of sequestering and *ad hoc* bulk soft terms, a perhaps more realistic alternative is mirage mediation (MM) models where gravity-mediated and anomaly-mediated soft terms are comparable. This class of models is expected to arise from IIB string compactification on an orientifold with moduli stabilization as in Kachru-Kallosh-Linde-Trivedi (KKLT) [135]; the dilaton S and complex structure moduli U^β are stabilized by fluxes and the Kähler moduli T^α are stabilized by nonperturbative effects such as gaugino condensation or instantons. While the S and U^β moduli are expected to gain Kaluza-Klein (KK) scale masses, the T^α moduli can be much lighter. Moduli stabilization leads to supersymmetric anti–de Sitter vacua, but uplifting of the scalar potential via addition of, for instance, an anti-D3 brane at the tip of a Klebanov-Strassler throat can lead to metastable deSitter vacua. A scale of hierarchies [82,136]

$$m_T \sim 4\pi^2 m_{3/2} \sim 4\pi^2 m_{\rm soft}$$

is expected to ensue, leading to comparable moduli and AMSB contributions to soft masses.

The original KKLT picture assumed a single Kähler modulus T and a simple uplift procedure. Within the MM model, the soft supersymmetry breaking (SSB) gaugino-mass parameters, trilinear SSB parameters and sfermion mass parameters, all renormalized just below the unification scale (taken to be $Q = m_{\rm GUT}$), are found to be [82],

$$M_a = M_s(l_a\alpha + b_a g_a^2), \tag{26}$$

$$A_{ijk} = M_s(-a_{ijk}\alpha + \gamma_i + \gamma_j + \gamma_k), \tag{27}$$

$$m_i^2 = M_s^2(c_i\alpha^2 + 4\alpha\xi_i - \dot\gamma_i), \tag{28}$$

where

$$M_s \equiv \frac{m_{3/2}}{16\pi^2},$$

b_a are the gauge β function coefficients for gauge group a and g_a are the corresponding gauge couplings. The coefficients that appear in (26)–(28) are given by

$$c_i = 1 - n_i,$$

$$a_{ijk} = 3 - n_i - n_j - n_k$$

and

$$\xi_i = \sum_{j,k} a_{ijk}\frac{y_{ijk}^2}{4} - \sum_a l_a g_a^2 C_2^a(f_i).$$

Finally, y_{ijk} are the superpotential Yukawa couplings, C_2^a is the quadratic Casimir for the ath gauge group corresponding to the representation to which the sfermion $\tilde f_i$ belongs, γ_i is the anomalous dimension and

$$\dot\gamma_i = 8\pi^2\frac{\partial\gamma_i}{\partial\log\mu}.$$

Expressions for the last two quantities involving the anomalous dimensions can be found in the Appendixes of Refs. [137,138]. The quantity l_a is the power of the modulus field entering the gauge kinetic function. The n_i are modular weights which take on discrete values in the original construction based on the brane locations of the matter superfields [82].

The MM model is then specified by the parameters

$$m_{3/2}, \alpha, \tan\beta, {\rm sign}(\mu), n_i, l_a. \tag{29}$$

The mass scale for the SSB parameters is dictated by the gravitino mass $m_{3/2}$. The phenomenological parameter α, which could be of either sign, determines the relative contributions of anomaly mediation and gravity mediation to the soft terms, and is expected to be $|\alpha| \sim \mathcal{O}(1)$. Grand unification implies matter particles within the same GUT multiplet have common modular weights, and that the l_a are universal. We will assume here that all $l_a = 1$ and, for simplicity, there is a common modular weight for all matter scalars c_m but we will allow for different modular weights c_{H_u} and c_{H_d} for each of the two Higgs doublets of the MSSM. Such choices for the scalar field modular weights are motivated for instance by $SO(10)$ SUSY GUT models where the MSSM Higgs doublets may live in different ten-dimensional Higgs reps.

For a variety of discrete parameter choices n_i, the various MM models have all been found to be unnatural when the Higgs mass m_h is restricted to be m_h: 123–127 GeV [45]. However, in Ref. [83], it was suggested that to allow for more realistic compactification schemes (wherein the Kähler moduli may number in the hundreds instead of just one) and for more diverse uplifting mechanisms, then the discrete valued parameter choices may be generalized to continuous ones. This transition to generalized MM models (GMM) then allows for natural models with $m_h \sim 125$ GeV. The parameter space of GMM is given by

$$\alpha, m_{3/2}, c_m, c_{m3}, a_3, c_{H_u}, c_{H_d}, \tan\beta \quad \text{(GMM)}, \qquad (30)$$

where a_3 is short for $a_{Q_3 H_u U_3}$ [appearing in Eq. (27)] and c_m, c_{m3}, c_{H_u}, and c_{H_d} arise in Eq. (28). Here, we adopt an independent value c_m for the first two matter-scalar generations whilst the parameter c_{m3} applies to third-generation matter scalars. The independent values of c_{H_u} and c_{H_d}, which set the moduli-mediated contribution to the soft Higgs mass-squared soft terms, may conveniently be traded for weak-scale values of μ and m_A as is done in the two-parameter nonuniversal Higgs model (NUHM2) [73];

$$\alpha, m_{3/2}, c_m, c_{m3}, a_3, \tan\beta, \mu, m_A \quad \text{(GMM}'\text{)}. \qquad (31)$$

This procedure allows for more direct exploration of stringy natural SUSY parameter space where most landscape solutions require $\mu \sim 100$–300 GeV in anthropically allowed pocket universes [139].

Thus, our final formulas for the soft terms are given by

$$M_a = (\alpha + b_a g_a^2) m_{3/2}/16\pi^2, \qquad (32)$$

$$A_\tau = (-a_3\alpha + \gamma_{L_3} + \gamma_{H_d} + \gamma_{E_3}) m_{3/2}/16\pi^2, \qquad (33)$$

$$A_b = (-a_3\alpha + \gamma_{Q_3} + \gamma_{H_d} + \gamma_{D_3}) m_{3/2}/16\pi^2, \qquad (34)$$

$$A_t = (-a_3\alpha + \gamma_{Q_3} + \gamma_{H_u} + \gamma_{U_3}) m_{3/2}/16\pi^2, \qquad (35)$$

$$m_i^2(1,2) = (c_m\alpha^2 + 4\alpha\xi_i - \dot{\gamma}_i)(m_{3/2}/16\pi^2)^2, \qquad (36)$$

$$m_j^2(3) = (c_{m3}\alpha^2 + 4\alpha\xi_j - \dot{\gamma}_j)(m_{3/2}/16\pi^2)^2, \qquad (37)$$

$$m_{H_u}^2 = (c_{H_u}\alpha^2 + 4\alpha\xi_{H_u} - \dot{\gamma}_{H_u})(m_{3/2}/16\pi^2)^2, \qquad (38)$$

$$m_{H_d}^2 = (c_{H_d}\alpha^2 + 4\alpha\xi_{H_d} - \dot{\gamma}_{H_d})(m_{3/2}/16\pi^2)^2, \qquad (39)$$

where, for a given value of α and $m_{3/2}$, the values of c_{H_u} and c_{H_d} are adjusted so as to fulfill the input values of μ and m_A. In the above expressions, the index i runs over first-/second-generation MSSM scalars $i = Q_{1,2}, U_{1,2}, D_{1,2}, L_{1,2}$, and $E_{1,2}$ while j runs overs third-generation scalars $j = Q_3$, U_3, D_3, L_3, and E_3. The natural GMM model has been incorporated into the event generator program Isajet 7.86 [126]. Here again, there is ambiguity in the evaluation of $\Delta_{\rm BG}$ and $\Delta_{\rm HS}$ while evaluation of $\Delta_{\rm EW}$ is unambiguous.

In Fig. 18, we show color-coded regions of $\Delta_{\rm EW}$ for the GMM′ model m_0^{MM} vs $m_{1/2}^{MM}$ plane for $a_3 = 1.6\sqrt{c_m}$, $c_m = c_{m3}$ and with $\mu = 200$ GeV and $m_A = 2000$ GeV. Here, m_0^{MM} is defined as

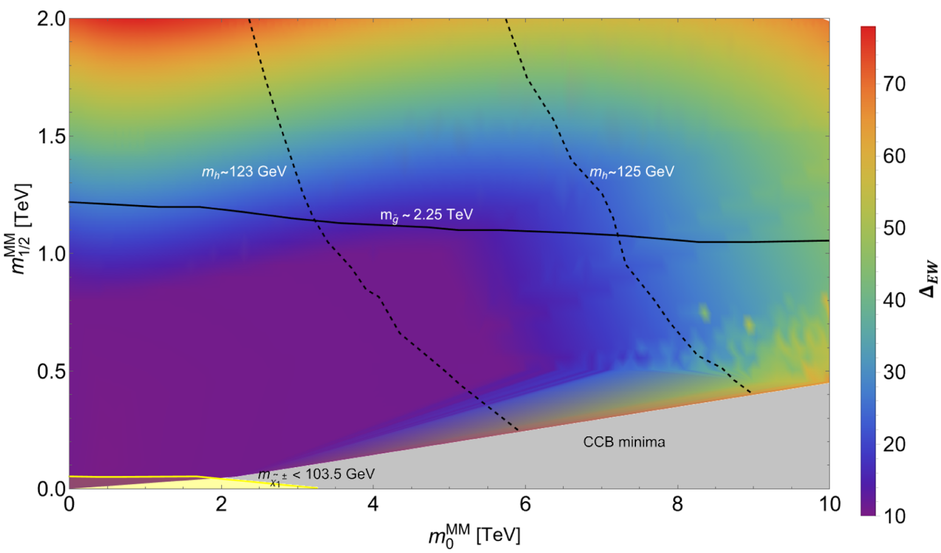

FIG. 18. Plot of naturalness measure $\Delta_{\rm EW}$ in the m_0^{MM} vs $m_{1/2}^{MM}$ plane of the generalized mirage-mediation model for $\tan\beta = 10$ with $c_m = c_{m3}$ and $a_3 = 1.6\sqrt{c_m}$. For GMM′, we also require $\mu = 200$ GeV and $m_A = 2$ TeV. The spectra are calculated using Isasugra.

$$m_0^{MM} = \sqrt{c_m}\alpha m_{3/2}/16\pi^2$$

and $m_{1/2}^{MM}$ as

$$m_{1/2}^{MM} = \alpha m_{3/2}/16\pi^2.$$

We also show contours of $m_h = 123$ GeV and 127 GeV and a contour of $m_{\tilde{g}} = 2.25$ TeV. The lower-right region is excluded due to CCB minima, while the yellow lower-left region has $m_{\tilde{\chi}_1^+} < 103.5$ GeV. From the plot, we see a vast purple- and blue-colored region with $\Delta_{\rm EW} \sim 10$–20; highly EW natural. Also, much of this region has a light Higgs scalar with mass $m_h \sim 125$ GeV. The key signature of GMM models is the fact that the gaugino masses should unify at scales well below $Q = m_{\rm GUT}$. Thus, if SUSY were discovered, a high-priority issue would be to measure $m_{\tilde{g}}$ (M_3) and $m_{\tilde{\chi}_2^+}$ (M_2) to determine the scale Q at which these values unify. A measurement of the bino mass M_1 would also be useful, but this may be more difficult than measuring M_3 and M_2.

IX. CONCLUSIONS

In this paper, we have reexamined three fine-tuning measures which are widely used in the literature: $\Delta_{\rm BG}$, $\Delta_{\rm HS}$, and $\Delta_{\rm EW}$. A fourth, stringy naturalness, does not yet admit a quantitative measure although it may be possible in future work. These measures have been quoted vaguely to bolster opinions on future HE facilities and to set policy for future experiments. Given these consequences, a critical evaluation seems necessary. While naturalness definitions such as 't Hooft naturalness certainly apply to supersymmetry and the big hierarchy problem, in that a low scale of SUSY breaking is technically natural (in that the model becomes more (super)symmetric as the SUSY breaking order parameter tends to zero) this doesn't apply to the little hierarchy problem (LHP) which is instead concerned with the increasing mass gap between the measured value of the weak scale and the scale of soft-SUSY breaking terms [which determine $m_{\rm weak}$ via Eq. (3)]. For the LHP, we invoke instead the notion of practical naturalness, where all independent contributions to any observable should be comparable to or less than the measured value of the observable.

The three naturalness measures are all attempts to measure practical naturalness. The $\Delta_{\rm EW}$ measure is most conservative and unavoidable. It is model independent within a fixed matter content (such as the MSSM). It is also unambiguous. Its lessons can be immediately extracted from Eq. (3); the only superparticles required at the weak scale are the various higgsinos whose mass derives from the SUSY conserving μ parameter. While the value of μ is frequently tuned in Eq. (3) such as to give the measured value of m_Z, its physics origin is rather obscure and may or may not be directly related to SUSY breaking.[9] Of the remaining superparticle contributions to the weak scale, all are suppressed by loop factors times mass-squared factors in Eq. (3) so that the sparticles can lie in the TeV to multi-TeV range at little cost to naturalness. In the string landscape picture, in fact, there is a statistical draw to large soft terms so long as their contributions to the weak scale are not too large. This then predicts $m_h \sim 125$ GeV with sparticles typically beyond present reach of the LHC [114,141].

The traditional $\Delta_{\rm BG}$ measure which instead famously placed upper bounds on all sparticles of just a few hundred GeV suffers from the ambiguity of what to take as free parameters in the log-derivative measure. While the commonly used SUSY EFTs adopt a variety of "parameters of ignorance", it is noted that in more specific models the soft terms are all correlated (in our universe). Taking multiple soft parameters as the p_i in $\Delta_{\rm BG}$ leads to overestimates of finetuning by factors of up to 500–1000 as compared to $\Delta_{\rm EW}$. Also, the measure $\Delta_{\rm BG}$ is rather complicated to compute, so we have embedded its numerical evaluation into the publicly available code DEW4SLHA which computes all three finetuning measures given an input SUSY Les Houches Accord file. By combining dependent soft terms, then $\Delta_{\rm BG}$ reduces to the tree-level value of $\Delta_{\rm EW}$.

The measure Δ_{HS} which evaluates to be approximately $\sim\delta m_{H_u}^2/m_{\rm weak}^2$ is found to overestimate fine-tuning by artificially splitting $m_{H_u}^2({\rm weak})$ into $m_{H_u}^2(\Lambda) + \delta m_{H_u}^2$. These are not independent contributions to m_h^2. In fact, selection of appropriately broken EW symmetry requires $\delta m_{H_u}^2$ to be large or else EW symmetry is not broken. This measure, which famously predicts three third-generation squarks below 500 GeV, also overestimates fine-tuning by up to three orders of magnitude. By combining the dependent terms $m_{H_u}^2(\Lambda)$ with $\delta m_{H_u}^2$, then $\Delta_{\rm HS}$ reduces to $\Delta_{\rm EW}$ according to Eq. (20).

Our ultimate conclusion is that the so-called naturalness crisis [142,143] which arose from non-observation of SUSY particles at LHC is not a crisis at all, but is based on faulty estimates of finetuning by the $\Delta_{\rm BG}$ and $\Delta_{\rm HS}$ measures (which are actually inconsistent with each other). The more conservative measure $\Delta_{\rm EW}$ rules out old favorites such as the CMSSM/mSUGRA, mAMSB, mGMSB, and MM models based on naturalness, but allows for plenty of natural parameter space in models like NUHMi, nAMSB, and nGMM (and of course less theoretically constrained exploratory constructs like pMSSM). In fact, the naturalness-allowed and LHC-allowed parameter space regions are precisely those which seem most prevalent from rather general considerations of the string landscape. In this light, the above natural SUSY models maintain a high degree of

[9] Twenty solutions to the SUSY μ problem are reviewed in Ref. [140].

motivation, and are perhaps even more highly motivated than pre-LHC times due to the emergence of the string landscape. Thus, policy decisions for future HEP facilities, especially future accelerators, should bear this resolution in mind in that it may be that we just need a much more energetic collider for the discovery of superpartners.

ACKNOWLEDGMENTS

This material is based upon work supported by the U.S. Department of Energy, Office of Science, Office of Basic Energy Sciences Energy Frontier Research Centers program under Award No. DE-SC-0009956 and U.S. Department of Energy Grant No. DE-SC-0017647.

[1] E. Witten, Dynamical breaking of supersymmetry, Nucl. Phys. **B188**, 513 (1981).
[2] R. K. Kaul, Gauge hierarchy in a supersymmetric model, Phys. Lett. **109B**, 19 (1982).
[3] S. Dimopoulos, S. Raby, and F. Wilczek, Supersymmetry and the scale of unification, Phys. Rev. D **24**, 1681 (1981).
[4] U. Amaldi, W. de Boer, and H. Furstenau, Comparison of grand unified theories with electroweak and strong coupling constants measured at LEP, Phys. Lett. B **260**, 447 (1991).
[5] J. R. Ellis, S. Kelley, and D. V. Nanopoulos, Probing the desert using gauge coupling unification, Phys. Lett. B **260**, 131 (1991).
[6] P. Langacker and M. Luo, Implications of precision electroweak experiments for M_t, ρ_0, $\sin^2\theta_W$ and grand unification, Phys. Rev. D **44**, 817 (1991).
[7] L. E. Ibanez and G. G. Ross, SU(2)-L x U(1) symmetry breaking as a radiative effect of supersymmetry breaking in guts, Phys. Lett. **110B**, 215 (1982).
[8] L. E. Ibanez and C. Lopez, $N = 1$ supergravity, the breaking of $\mathrm{SU}(2) \times \mathrm{U}(1)$ and the top quark mass, Phys. Lett. **126B**, 54 (1983).
[9] L. Alvarez-Gaume, J. Polchinski, and M. B. Wise, Minimal low-energy supergravity, Nucl. Phys. **B221**, 495 (1983).
[10] P. Slavich *et al.*, Higgs-mass predictions in the MSSM and beyond, Eur. Phys. J. C **81**, 450 (2021).
[11] S. Heinemeyer, W. Hollik, G. Weiglein, and L. Zeune, Implications of LHC search results on the W boson mass prediction in the MSSM, J. High Energy Phys. 12 (2013) 084.
[12] P. Candelas, G. T. Horowitz, A. Strominger, and E. Witten, Vacuum configurations for superstrings, Nucl. Phys. **B258**, 46 (1985).
[13] B. S. Acharya, Supersymmetry, Ricci flat manifolds and the string landscape, J. High Energy Phys. 08 (2020) 128.
[14] J. R. Ellis and D. Ross, A light Higgs boson would invite supersymmetry, Phys. Lett. B **506**, 331 (2001).
[15] F. Vissani, Do experiments suggest a hierarchy problem?, Phys. Rev. D **57**, 7027 (1998).
[16] M. Farina, D. Pappadopulo, and A. Strumia, A modified naturalness principle and its experimental tests, J. High Energy Phys. 08 (2013) 022.
[17] C. K. M. Klein, Minimal radiative neutrino mass -A systematic study-, Master's thesis, Heidelberg, Max Planck institute, 2019.
[18] H. M. Lee, S. Raby, M. Ratz, G. G. Ross, R. Schieren, K. Schmidt-Hoberg, and P. K. S. Vaudrevange, Discrete R symmetries for the MSSM and its singlet extensions, Nucl. Phys. **B850**, 1 (2011).
[19] H. P. Nilles, Stringy origin of discrete R-symmetries, Proc. Sci. CORFU2016 (**2017**) 017.
[20] H. Baer, V. Barger, and D. Sengupta, Gravity safe, electroweak natural axionic solution to strong *CP* and SUSY μ problems, Phys. Lett. B **790**, 58 (2019).
[21] P. N. Bhattiprolu and S. P. Martin, High-quality axions in solutions to the μ problem, Phys. Rev. D **104**, 055014 (2021).
[22] M. Demirtas, N. Gendler, C. Long, L. McAllister, and J. Moritz, PQ axiverse, J. High Energy Phys. 06 (2023) 092.
[23] M. Dine and A. Kusenko, The origin of the matter—antimatter asymmetry, Rev. Mod. Phys. **76**, 1 (2003).
[24] K. J. Bae, H. Baer, H. Serce, and Y.-F. Zhang, Leptogenesis scenarios for natural SUSY with mixed axion-higgsino dark matter, J. Cosmol. Astropart. Phys. 01 (2016) 012.
[25] H. Baer and X. Tata, *Weak Scale Supersymmetry: From Superfields to Scattering Events* (Cambridge University Press, Cambridge, England, 2006).
[26] N. Craig *et al.*, Snowmass theory frontier report, arXiv:2211.05772.
[27] M. Narain *et al.*, The future of US particle physics—the snowmass 2021 energy frontier report, arXiv:2211.11084.
[28] J. R. Ellis, K. Enqvist, D. V. Nanopoulos, and F. Zwirner, Observables in low-energy superstring models, Mod. Phys. Lett. A **01**, 57 (1986).
[29] R. Barbieri and G. F. Giudice, Upper bounds on supersymmetric particle masses, Nucl. Phys. **B306**, 63 (1988).
[30] B. de Carlos and J. A. Casas, One loop analysis of the electroweak breaking in supersymmetric models and the fine tuning problem, Phys. Lett. B **309**, 320 (1993).
[31] G. W. Anderson and D. J. Castano, Naturalness and superpartner masses or when to give up on weak scale supersymmetry, Phys. Rev. D **52**, 1693 (1995).
[32] S. Dimopoulos and G. F. Giudice, Naturalness constraints in supersymmetric theories with nonuniversal soft terms, Phys. Lett. B **357**, 573 (1995).
[33] P. H. Chankowski, J. R. Ellis, and S. Pokorski, The fine tuning price of LEP, Phys. Lett. B **423**, 327 (1998).
[34] P. H. Chankowski, J. R. Ellis, M. Olechowski, and S. Pokorski, Haggling over the fine tuning price of LEP, Nucl. Phys. **B544**, 39 (1999).

[35] M. Bastero-Gil, G. L. Kane, and S. F. King, Fine tuning constraints on supergravity models, Phys. Lett. B **474**, 103 (2000).
[36] H. Abe, T. Kobayashi, and Y. Omura, Relaxed fine-tuning in models with non-universal gaugino masses, Phys. Rev. D **76**, 015002 (2007).
[37] R. K. Ellis *et al.*, Physics briefing book: Input for the european strategy for particle physics update 2020, arXiv:1910.11775.
[38] J. N. Butler *et al.*, Report of the 2021 U.S. Community Study on the Future of Particle Physics (Snowmass 2021) (2023), 10.2172/1922503.
[39] L. Susskind, Dynamics of spontaneous symmetry breaking in the Weinberg-Salam theory, Phys. Rev. D **20**, 2619 (1979).
[40] J. L. Feng, K. T. Matchev, and T. Moroi, Multi—TeV Scalars are Natural in Minimal Supergravity, Phys. Rev. Lett. **84**, 2322 (2000).
[41] J. L. Feng, K. T. Matchev, and T. Moroi, Focus points and naturalness in supersymmetry, Phys. Rev. D **61**, 075005 (2000).
[42] R. L. Arnowitt and P. Nath, Supersymmetry and supergravity: Phenomenology and grand unification, in *Proceedings of the 6th Summer School Jorge Andre Swieca on Nuclear Physics* (1993), arXiv:hep-ph/9309277.
[43] G. L. Kane, C. F. Kolda, L. Roszkowski, and J. D. Wells, Study of constrained minimal supersymmetry, Phys. Rev. D **49**, 6173 (1994).
[44] H. Baer, V. Barger, and D. Mickelson, How conventional measures overestimate electroweak fine-tuning in supersymmetric theory, Phys. Rev. D **88**, 095013 (2013).
[45] H. Baer, V. Barger, D. Mickelson, and M. Padeffke-Kirkland, SUSY models under siege: LHC constraints and electroweak fine-tuning, Phys. Rev. D **89**, 115019 (2014).
[46] H. Murayama, Supersymmetry phenomenology, in *ICTP Summer School in Particle Physics* (2000), pp. 296–335, arXiv:hep-ph/0002232.
[47] R. Harnik, G. D. Kribs, D. T. Larson, and H. Murayama, The minimal supersymmetric fat Higgs model, Phys. Rev. D **70**, 015002 (2004).
[48] Z. Chacko, Y. Nomura, and D. Tucker-Smith, A minimally fine-tuned supersymmetric standard model, Nucl. Phys. **B725**, 207 (2005).
[49] R. Kitano and Y. Nomura, A solution to the supersymmetric fine-tuning problem within the MSSM, Phys. Lett. B **631**, 58 (2005).
[50] R. Kitano and Y. Nomura, Supersymmetry, naturalness, and signatures at the LHC, Phys. Rev. D **73**, 095004 (2006).
[51] M. Papucci, J. T. Ruderman, and A. Weiler, Natural SUSY endures, J. High Energy Phys. 09 (2012) 035.
[52] C. Brust, A. Katz, S. Lawrence, and R. Sundrum, SUSY, the third generation and the LHC, J. High Energy Phys. 03 (2012) 103.
[53] H. Baer, V. Barger, P. Huang, A. Mustafayev, and X. Tata, Radiative Natural SUSY with a 125 GeV Higgs Boson, Phys. Rev. Lett. **109**, 161802 (2012).
[54] H. Baer, V. Barger, and D. Martinez, Comparison of SUSY spectra generators for natural SUSY and string landscape predictions, Eur. Phys. J. C **82**, 172 (2022).
[55] K. L. Chan, U. Chattopadhyay, and P. Nath, Naturalness, weak scale supersymmetry and the prospect for the observation of supersymmetry at the Tevatron and at the CERN LHC, Phys. Rev. D **58**, 096004 (1998).
[56] M. R. Douglas, Basic results in vacuum statistics, C.R. Phys. **5**, 965 (2004).
[57] V. Agrawal, S. M. Barr, J. F. Donoghue, and D. Seckel, Viable range of the mass scale of the Standard Model, Phys. Rev. D **57**, 5480 (1998).
[58] H. Baer, V. Barger, and S. Salam, Naturalness versus stringy naturalness (with implications for collider and dark matter searches), Phys. Rev. Res. **1**, 023001 (2019).
[59] P. Z. Skands *et al.*, SUSY Les Houches accord: Interfacing SUSY spectrum calculators, decay packages, and event generators, J. High Energy Phys. 07 (2004) 036.
[60] R. L. Workman *et al.*, Review of particle physics, Prog. Theor. Exp. Phys. **2022**, 083C01 (2022).
[61] M. Drees and M. M. Nojiri, Radiative symmetry breaking in minimal $N = 1$ supergravity with large Yukawa couplings, Nucl. Phys. **B369**, 54 (1992).
[62] S. Kelley, J. L. Lopez, D. V. Nanopoulos, H. Pois, and K.-j. Yuan, No scale supergravity confronts experiment, Phys. Lett. B **273**, 423 (1991).
[63] S. Kelley, J. L. Lopez, D. V. Nanopoulos, H. Pois, and K.-j. Yuan, Aspects of radiative electroweak breaking in supergravity models, Nucl. Phys. **B398**, 3 (1993).
[64] P. Nath and R. L. Arnowitt, Predictions in SU(5) Supergravity Grand Unification with Proton Stability and Relic Density Constraints, Phys. Rev. Lett. **70**, 3696 (1993).
[65] V. D. Barger, M. S. Berger, and P. Ohmann, The supersymmetric particle spectrum, Phys. Rev. D **49**, 4908 (1994).
[66] S. K. Soni and H. A. Weldon, Analysis of the supersymmetry breaking induced by $N = 1$ supergravity theories, Phys. Lett. **126B**, 215 (1983).
[67] V. S. Kaplunovsky and J. Louis, Model independent analysis of soft terms in effective supergravity and in string theory, Phys. Lett. B **306**, 269 (1993).
[68] A. Brignole, L. E. Ibanez, and C. Munoz, Towards a theory of soft terms for the supersymmetric standard model, Nucl. Phys. **B422**, 125 (1994); Nucl. Phys. **B436**, 747(E) (1995).
[69] F. Gabbiani, E. Gabrielli, A. Masiero, and L. Silvestrini, A complete analysis of FCNC and *CP* constraints in general SUSY extensions of the standard model, Nucl. Phys. **B477**, 321 (1996).
[70] H. Baer, A. Mustafayev, S. Profumo, A. Belyaev, and X. Tata, Neutralino cold dark matter in a one parameter extension of the minimal supergravity model, Phys. Rev. D **71**, 095008 (2005).
[71] J. R. Ellis, K. A. Olive, and Y. Santoso, The MSSM parameter space with nonuniversal Higgs masses, Phys. Lett. B **539**, 107 (2002).
[72] J. R. Ellis, T. Falk, K. A. Olive, and Y. Santoso, Exploration of the MSSM with nonuniversal Higgs masses, Nucl. Phys. **B652**, 259 (2003).
[73] H. Baer, A. Mustafayev, S. Profumo, A. Belyaev, and X. Tata, Direct, indirect and collider detection of neutralino dark matter in SUSY models with non-universal Higgs masses, J. High Energy Phys. 07 (2005) 065.
[74] W. Buchmuller, K. Hamaguchi, O. Lebedev, and M. Ratz, Local grand unification, in *Proceedings of the*

GUSTAVOFEST: Symposium in Honor of Gustavo C. Branco: CP Violation and the Flavor Puzzle (2005), pp. 143–156, arXiv:hep-ph/0512326.
[75] H. P. Nilles, S. Ramos-Sanchez, and P. K. S. Vaudrevange, Local grand unification and string theory, AIP Conf. Proc. **1200**, 226 (2010).
[76] H. P. Nilles and P. K. S. Vaudrevange, Geography of fields in extra dimensions: String theory lessons for particle physics, Mod. Phys. Lett. A **30**, 1530008 (2015).
[77] A. Pomarol and D. Tommasini, Horizontal symmetries for the supersymmetric flavor problem, Nucl. Phys. **B466**, 3 (1996).
[78] H. Baer, V. Barger, and D. Sengupta, Landscape solution to the SUSY flavor and *CP* problems, Phys. Rev. Res. **1**, 033179 (2019).
[79] L. Randall and R. Sundrum, Out of this world supersymmetry breaking, Nucl. Phys. **B557**, 79 (1999).
[80] G. F. Giudice, M. A. Luty, H. Murayama, and R. Rattazzi, Gaugino mass without singlets, J. High Energy Phys. 12 (1998) 027.
[81] H. Baer, V. Barger, and D. Sengupta, Anomaly mediated SUSY breaking model retrofitted for naturalness, Phys. Rev. D **98**, 015039 (2018).
[82] K. Choi, A. Falkowski, H. P. Nilles, and M. Olechowski, Soft supersymmetry breaking in KKLT flux compactification, Nucl. Phys. **B718**, 113 (2005).
[83] H. Baer, V. Barger, H. Serce, and X. Tata, Natural generalized mirage mediation, Phys. Rev. D **94**, 115017 (2016).
[84] G. 't Hooft, Naturalness, chiral symmetry, and spontaneous chiral symmetry breaking, NATO Sci. Ser. B **59**, 135 (1980).
[85] R. Barbieri and A. Strumia, The 'LEP paradox', in *Proceedings of the 4th Rencontres du Vietnam*: Physics at Extreme Energies (Particle Physics and Astrophysics) (2000), arXiv:hep-ph/0007265.
[86] A. Birkedal, Z. Chacko, and M. K. Gaillard, Little supersymmetry and the supersymmetric little hierarchy problem, J. High Energy Phys. 10 (2004) 036.
[87] A. Canepa, Searches for supersymmetry at the large hadron collider, Rev. Phys. **4**, 100033 (2019).
[88] H. Baer, V. Barger, and M. Savoy, Upper bounds on sparticle masses from naturalness or how to disprove weak scale supersymmetry, Phys. Rev. D **93**, 035016 (2016).
[89] M. J. G. Veltman, The infrared—ultraviolet connection, Acta Phys. Pol. B **12**, 437 (1981).
[90] M. K. Gaillard and B. W. Lee, Rare decay modes of the K-mesons in gauge theories, Phys. Rev. D **10**, 897 (1974).
[91] J. L. Feng, Naturalness and the status of supersymmetry, Annu. Rev. Nucl. Part. Sci. **63**, 351 (2013).
[92] G. F. Giudice, Naturally speaking: The naturalness criterion and physics at the LHC (2008), pp. 155–178, arXiv: 0801.2562.
[93] L. E. Ibanez, C. Lopez, and C. Munoz, The low-energy supersymmetric spectrum according to $N = 1$ supergravity guts, Nucl. Phys. **B256**, 218 (1985).
[94] A. Lleyda and C. Munoz, Nonuniversal soft scalar masses in supersymmetric theories, Phys. Lett. B **317**, 82 (1993).
[95] S. P. Martin, Compressed supersymmetry and natural neutralino dark matter from top squark-mediated annihilation to top quarks, Phys. Rev. D **75**, 115005 (2007).
[96] S. P. Martin and M. T. Vaughn, Two loop renormalization group equations for soft supersymmetry breaking couplings, Phys. Rev. D **50**, 2282 (1994); Phys. Rev. D **78**, 039903(E) (2008).
[97] B. C. Allanach, J. P. J. Hetherington, M. A. Parker, and B. R. Webber, Naturalness reach of the large hadron collider in minimal supergravity, J. High Energy Phys. 08 (2000) 017.
[98] M. T. Grisaru, W. Siegel, and M. Roček, Improved methods for supergraphs, Nucl. Phys. **B159**, 429 (1979).
[99] K. J. Bae, H. Baer, N. Nagata, and H. Serce, Prospects for Higgs coupling measurements in SUSY with radiatively-driven naturalness, Phys. Rev. D **92**, 035006 (2015).
[100] H. Baer, V. Barger, P. Huang, D. Mickelson, A. Mustafayev, and X. Tata, Post-LHC7 fine-tuning in the minimal supergravity/CMSSM model with a 125 GeV Higgs boson, Phys. Rev. D **87**, 035017 (2013).
[101] H. Baer, V. Barger, and M. Savoy, Supergravity gauge theories strike back: There is no crisis for SUSY but a new collider may be required for discovery, Phys. Scr. **90**, 068003 (2015).
[102] H. Baer, V. Barger, M. Savoy, and H. Serce, The Higgs mass and natural supersymmetric spectrum from the landscape, Phys. Lett. B **758**, 113 (2016).
[103] H. Baer, K.-Y. Choi, J. E. Kim, and L. Roszkowski, Dark matter production in the early Universe: Beyond the thermal WIMP paradigm, Phys. Rep. **555**, 1 (2015).
[104] K. J. Bae, H. Baer, and E. J. Chun, Mixed axion/neutralino dark matter in the SUSY DFSZ axion model, J. Cosmol. Astropart. Phys. 12 (2013) 028.
[105] H. Baer, V. Barger, and R. Wiley Deal, Dark matter and dark radiation from the early universe with a modulus coupled to the PQMSSM, J. High Energy Phys. 06 (2023) 083.
[106] K. J. Bae, H. Baer, and E. J. Chun, Mainly axion cold dark matter from natural supersymmetry, Phys. Rev. D **89**, 031701 (2014).
[107] H. Baer, V. Barger, P. Huang, D. Mickelson, A. Mustafayev, and X. Tata, Radiative natural supersymmetry: Reconciling electroweak fine-tuning and the Higgs boson mass, Phys. Rev. D **87**, 115028 (2013).
[108] A. Dedes and P. Slavich, Two loop corrections to radiative electroweak symmetry breaking in the MSSM, Nucl. Phys. **B657**, 333 (2003).
[109] H. Baer, V. Barger, J. S. Gainer, H. Serce, and X. Tata, Reach of the high-energy LHC for gluinos and top squarks in SUSY models with light Higgsinos, Phys. Rev. D **96**, 115008 (2017).
[110] M. van Beekveld, W. Beenakker, S. Caron, R. Peeters, and R. Ruiz de Austri, Supersymmetry with dark matter is still natural, Phys. Rev. D **96**, 035015 (2017).
[111] M. van Beekveld, S. Caron, and R. Ruiz de Austri, The current status of fine-tuning in supersymmetry, J. High Energy Phys. 01 (2020) 147.
[112] H. Baer, V. Barger, S. Salam, and H. Serce, Supersymmetric particle and Higgs boson masses from the landscape: Dynamical versus spontaneous supersymmetry breaking, Phys. Rev. D **104**, 115025 (2021).
[113] M. R. Douglas, Statistical analysis of the supersymmetry breaking scale, arXiv:hep-th/0405279.

[114] H. Baer, V. Barger, H. Serce, and K. Sinha, Higgs and superparticle mass predictions from the landscape, J. High Energy Phys. 03 (2018) 002.
[115] G. F. Giudice and R. Rattazzi, Living dangerously with low-energy supersymmetry, Nucl. Phys. **B757**, 19 (2006).
[116] N. Arkani-Hamed, S. Dimopoulos, and S. Kachru, Predictive landscapes and new physics at a TeV, arXiv:hep-th/0501082.
[117] B. C. Allanach, SOFTSUSY: A program for calculating supersymmetric spectra, Comput. Phys. Commun. **143**, 305 (2002).
[118] N. Arkani-Hamed, A. Delgado, and G. F. Giudice, The well-tempered neutralino, Nucl. Phys. **B741**, 108 (2006).
[119] H. Baer, A. Mustafayev, E.-K. Park, and X. Tata, Target dark matter detection rates in models with a well-tempered neutralino, J. Cosmol. Astropart. Phys. 01 (2007) 017.
[120] H. Baer, V. Barger, and H. Serce, SUSY under siege from direct and indirect WIMP detection experiments, Phys. Rev. D **94**, 115019 (2016).
[121] M. Badziak, M. Olechowski, and P. Szczerbiak, Is well-tempered neutralino in MSSM still alive after 2016 LUX results?, Phys. Lett. B **770**, 226 (2017).
[122] S. Profumo, T. Stefaniak, and L. Stephenson Haskins, The not-so-well tempered neutralino, Phys. Rev. D **96**, 055018 (2017).
[123] E. Aprile *et al.*, Dark Matter Search Results from a One Ton-Year Exposure of XENON1T, Phys. Rev. Lett. **121**, 111302 (2018).
[124] J. Aalbers *et al.*, First Dark Matter Search Results from the LUX-ZEPLIN (LZ) Experiment, Phys. Rev. Lett. **131**, 041002 (2023).
[125] H. Bahl, T. Hahn, S. Heinemeyer, W. Hollik, S. Paßehr, H. Rzehak, and G. Weiglein, Precision calculations in the MSSM Higgs-boson sector with FeynHiggs 2.14, Comput. Phys. Commun. **249**, 107099 (2020).
[126] F. E. Paige, S. D. Protopopescu, H. Baer, and X. Tata, ISAJET 7.69: A Monte Carlo event generator for pp, $\bar{p}p$, and e^+e^- reactions, arXiv:hep-ph/0312045.
[127] T. Gherghetta, G. F. Giudice, and J. D. Wells, Phenomenological consequences of supersymmetry with anomaly induced masses, Nucl. Phys. **B559**, 27 (1999).
[128] J. L. Feng and T. Moroi, Supernatural supersymmetry: Phenomenological implications of anomaly mediated supersymmetry breaking, Phys. Rev. D **61**, 095004 (2000).
[129] T. Cohen, M. Lisanti, A. Pierce, and T. R. Slatyer, Wino dark matter under siege, J. Cosmol. Astropart. Phys. 10 (2013) 061.
[130] J. Fan and M. Reece, In wino veritas? Indirect searches shed light on neutralino dark matter, J. High Energy Phys. 10 (2013) 124.
[131] A. Arbey, M. Battaglia, A. Djouadi, F. Mahmoudi, and J. Quevillon, Implications of a 125 GeV Higgs for supersymmetric models, Phys. Lett. B **708**, 162 (2012).
[132] H. Baer, V. Barger, and A. Mustafayev, Neutralino dark matter in mSUGRA/CMSSM with a 125 GeV light Higgs scalar, J. High Energy Phys. 05 (2012) 091.
[133] J. D. Wells, PeV-scale supersymmetry, Phys. Rev. D **71**, 015013 (2005).
[134] N. Arkani-Hamed, S. Dimopoulos, G. F. Giudice, and A. Romanino, Aspects of split supersymmetry, Nucl. Phys. **B709**, 3 (2005).
[135] S. Kachru, R. Kallosh, A. D. Linde, and S. P. Trivedi, De Sitter vacua in string theory, Phys. Rev. D **68**, 046005 (2003).
[136] K. Choi, A. Falkowski, H. P. Nilles, M. Olechowski, and S. Pokorski, Stability of flux compactifications and the pattern of supersymmetry breaking, J. High Energy Phys. 11 (2004) 076.
[137] A. Falkowski, O. Lebedev, and Y. Mambrini, SUSY phenomenology of KKLT flux compactifications, J. High Energy Phys. 11 (2005) 034.
[138] K. Choi, K. S. Jeong, T. Kobayashi, and K.-i. Okumura, TeV scale mirage mediation and natural little SUSY hierarchy, Phys. Rev. D **75**, 095012 (2007).
[139] H. Baer, V. Barger, and D. Sengupta, Mirage mediation from the landscape, Phys. Rev. Res. **2**, 013346 (2020).
[140] K. J. Bae, H. Baer, V. Barger, and D. Sengupta, Revisiting the SUSY μ problem and its solutions in the LHC era, Phys. Rev. D **99**, 115027 (2019).
[141] H. Baer, V. Barger, S. Salam, D. Sengupta, and K. Sinha, Status of weak scale supersymmetry after LHC Run 2 and ton-scale noble liquid WIMP searches, Eur. Phys. J. Spec. Top. **229**, 3085 (2020).
[142] J. Lykken and M. Spiropulu, Supersymmetry and the crisis in physics, Sci. Am. **310**, No. 5, 36 (2014).
[143] M. Dine, Naturalness under stress, Annu. Rev. Nucl. Part. Sci. **65**, 43 (2015).